Journal of Soil Science and Plant Nutrition (2025) 25:4091–4111
https://doi.org/10.1007/s42729-025-02386-z

ORIGINAL PAPER

Mitigating Arsenate-Induced Phytotoxicity in Fenugreek Seedlings Using Garlic Extract: Insights into Photosynthesis, Arsenate Uptake, Antioxidative Machinery and Ultrastructure

Gehad A. Ragab[1] · **Khalil M. Saad-Allah**[1] · **Afaf A. Nessem**[1]

Received: 5 June 2024 / Accepted: 13 March 2025 / Published online: 10 April 2025
© The Author(s) 2025

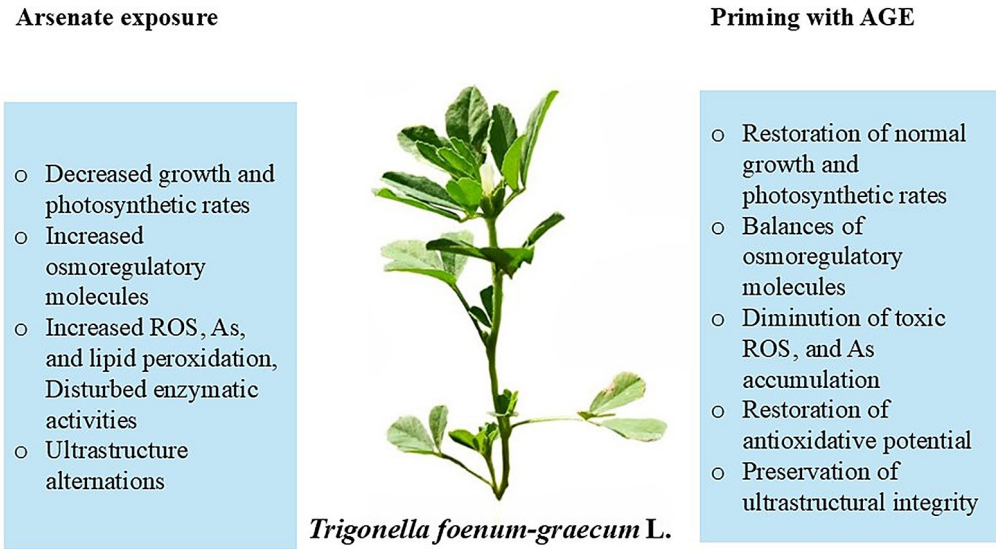
Abstract

Arsenate (As) pollution poses severe health issues due to its non-essentiality and mobility through food chains. The current investigation was conducted to study the stimulating capacity of aqueous garlic extract (AGE) to impede As toxicity in fenugreek (*Trigonella foenum-graecum* L.). Gas Chromatography-Mass Spectrometry (GC/MS) analysis of AGE revealed the presence of organosulfur and phenolic compounds. The irrigation with 50 mM As hampered the morphological, physiological, and biochemical traits of fenugreek. As-induced toxicity increased levels of hydrogen peroxide (H_2O_2), hydroxyl radical ($OH^{\bullet}$), and lipid peroxidation. The modified antioxidative machinery and increased osmolyte levels (amino acids, proline, and glycine betaine) were recorded following As application. Furthermore, As disrupted the ultrastructure of chloroplasts, mitochondria, cellular membranes, cell walls, and xylem vessels. AGE priming reduced As accumulation and restored plant growth, photosynthetic traits, and metabolic constituents. The antioxidative potential of AGE bioactive components upregulated enzymatic and non-enzymatic antioxidants and maintained the normal cell redox status of As-stressed fenugreek plants. Furthermore, AGE priming promoted superoxide dismutase (SOD) and ascorbate peroxidase (APOX) activities, limiting reactive oxygen species burst and membrane leakage. Additionally, AGE priming effectively restored normal ultrastructural compartments and cellular turgidity, preventing cell apoptotic symptoms and reducing As-induced cellular toxicity. The stimulatory potential of AGE can be assigned to its antioxidant components, which reduce oxidative stress and boost ROS detoxification mechanisms including the ascorbate–glutathione (ASA-GSH) cycle. Thus, As negatively impacted fenugreek, increased oxidative stress and disrupted cellular structures, but AGE priming countered As effects by enhancing antioxidants and cellular integrity, supporting plant recovery.

✉ Khalil M. Saad-Allah
khalil.saadallah@science.tanta.edu.eg

[1] Botany Department, Faculty of Science, Tanta University, Tanta 31527, Egypt

Graphical Abstract



Keywords Metal stress · Stress mitigation · Redox homeostasis · Lipid peroxidation · Sub-cellular compartments · Cellular deterioration

1 Introduction

Soil and water contamination with arsenic (As) is tremendously spread as a major environmental concern due to its increased release by natural and anthropogenic activities (Fatima et al. 2020). Moreover, As is a toxic metalloid that infiltrates agricultural systems through the broad usage of several industrial products such as fertilizers, herbicides, and pesticides (Li et al. 2021; Thakur et al. 2020). Being non-biologically degradable, the induced As accumulation in agricultural soils and plant tissues results in its entry into the food chain (Farouk and Al-Amri 2019; Saleem et al. 2023). An acute toxicity and carcinogenicity impact was harshly recorded even at low As doses, posing a severe danger to human health (Abbas et al. 2018; Seleem et al. 2021). The As toxicity received great attention due to its responsibility for chronic diseases such as gall bladder, lung, prostate, and skin cancers (Li et al. 2018).

The level of As contamination in agricultural soils is distressingly rising impairing soil quality, and plant metabolic activities including photosynthesis, transpiration, respiration, and yield (Ahmad et al. 2022; Fatima et al. 2020). It is a non-essential redox-active metalloid that appears in two inorganic forms; arsenate (V) occurring in the aerobic environment and arsenite (III) which is available under anaerobic conditions (Gąsecka et al. 2021). The conversion between these two oxidation states leads to higher production of reactive oxygen species (ROS) resulting in cellular disturbance of membranes and macromolecules (Mishra et al. 2021; Yadav et al. 2024). The triggered oxidative stress is counteracted by enzymatic defense antioxidants including superoxide dismutase, catalase, peroxidases, and enzymes of the glutathione-ascorbate (GSH-ASA) cycle. The non-enzymatic antioxidants comprise various compounds such as phenolics, flavonoids, carotenoids, ASA, and GSH (Kasim et al. 2014; Ragab and Saad-Allah 2021). Both ascorbate and glutathione are the main constituents of the ASC-GSH cycle, which are involved in ROS scavenging in chloroplasts and cytosol (Karam et al. 2017). Therefore, the ultimate toxicity of As is attributed to the metamorphosis in the ultrastructure of organelles and impairing normal metabolic activities (Du et al. 2017). However, various studies have screened As toxicity in several plants, and the mechanisms of its cellular damages, tolerance, and detoxifications in plants are not well investigated and need to deepen.

Instead of synthetic chemicals, biostimulants could be utilized as a green eco-friendly application to regulate and improve plant growth enhancing its stress resistance (Alkharpotly et al. 2024; Kutasy et al. 2023; Sharma et al. 2014). Biostimulants are extracts derived from natural sources that contain a diverse array of biologically active substances (Bulgari et al. 2015). Plant-derived biostimulants are widely applied in sustainable agriculture to improve nutrient use efficiency and enhance plant growth and development (Luziatelli et al. 2019). Among plant-derived biostimulants, garlic (*Allium sativum* L.) aqueous extract is known for its broad-spectrum antimicrobial properties and could alleviate pathogenic infections (Hayat et

al. 2018a). Furthermore, cultivating garlic with other crops exhibited a precious ability to counteract various biological and environmental stresses (Hayat et al. 2020). The usage of aqueous garlic extract enhanced plant growth, physiological characteristics, and phytochemical contents of many crops such as eggplants, snap beans, lettuce, tomato, and olive trees (Golubkina et al. 2024; Kutasy et al. 2023; Zulfiqar et al. 2020). Priming with garlic extract has been recently used to enhance plant responses to environmental constraints (Hayat et al. 2020; Kasim et al. 2017b). Although several studies investigated the substantial impact of many biostimulants with diverse chemical and biological components, limited literature focused on garlic extract application.

Fenugreek (*Trigonella foenum-graecum* L.) is a commonly cultivated plant renowned for its high nutritional properties across several nations (Xalxo and Keshavkant 2020). The significance of its cultivation relates to its versatile application as a spice in culinary practices and as a therapeutic agent in medicine, possessing analgesic, antidiabetic, and anti-inflammatory properties, along with substantial quantities of niacin, ASA, protein, and potassium (Alaraidh et al. 2018; Tufail et al. 2020). The expansion of fenugreek cultivation and the exploration of innovative approaches to enhance its resilience against environmental challenges are imperative for optimizing productivity and fortifying its adaptability. To the authors' knowledge, there is a dearth of literature regarding the precise mechanism underlying the use of garlic extract to improve plant responses to metal stress. Furthermore, although garlic extract possesses the potential to enhance plant resilience and tolerance to a variety of environmental stresses, there is a dearth of research on the specific mechanism through which it operates in this context. The current work might provide insights into the specific mechanisms and beneficial effects of seed priming with garlic extract in improving fenugreek responses to arsenate stress. In light of this, the present investigation seeks to investigate the morphological, biochemical, subcellular, and ultrastructural effects of arsenate on fenugreek seedlings. In addition, the study endeavors to evaluate the potential benefits of employing aqueous garlic extract as a seed bio-priming treatment in order to enhance plant resistance to arsenate-induced toxicity.

2 Materials and Methods

2.1 Preparation of Aqueous Garlic Extract and Determining Its Bioactive Constituents

The fresh garlic cloves were purchased from a local market and the bulbs were selected for their uniform size and appearance. The aqueous garlic extract (AGE) was prepared according to (Kasim et al. 2017b) with slight modifications. Briefly, a known weight of clean-washed bulbs was crushed and extracted in distilled water using a blender to obtain 25% (w/v). The crude extract was centrifuged at 5,000 rpm for 20 min. and the supernatant was collected, centrifugated, and filtered through filter paper (Whatman No.1). The freshly obtained AGE was immediately utilized as a seed priming application to avoid the disruption of bioactivity.

To determine the chemical composition of the AGE, a gas chromatograph/mass spectrometer (GC/MS) model Clarus 580/560S (PerkinElmer, Inc., Waltham, MA, USA) was utilized. The GC analysis employed an Elite-5MS column with dimensions of 30 m × 0.25 mm × 0.25 µm film thickness. The oven temperature was initially set at 80 °C for 7 min., followed by a ramp rate of 10 °C/min. to 140 °C, where it was held for 1 min. Subsequently, the temperature was increased to 200 °C at a rate of 10 °C/min. and held for 1 min., before reaching a final temperature of 280 °C at a rate of 5 °C/min. and held for 10 min. The transfer and input lines were maintained at a temperature of 250 °C. Helium gas was used as the carrier gas, flowing at a constant rate of 1 ml/min. The Autosampler AS3000 and a split mode (1:20) were employed, with an automatic injection of 1 µl sample volume after a solvent delay of 5 min. Electron ionization (EI) mass spectra were obtained at an ionization energy of 70 eV, at the range of 40–650 m/z in full scan mode. The ionization chamber temperature was fixed at 200 °C. The retention times and mass spectra of the obtained components were compared to those present in the WILEY 09, replib, and NIST 11 mass spectral databases (Hossain et al. 2011; NIST 2014; Oberacher 2012; Sharma et al. 2022) to identify and characterize each constituent of the analyzed AGE. The phytohormones (gibberellic acid, indole 3-acetic acid, abscisic acid,, and cytokinins) of GAE were quantified according to the methodology of Shindy and Smith (1975). Elemental analysis was performed via the combined acid-digestion method as described by Allen et al. (1974), with the contents of P, Ca, Mg, Fe, Mn, Zn, Cu, Mo, and Se quantified using inductively coupled plasma (ICP) spectrometry (Ultima 2 JY). The determination of S and N was conducted using the Kjeldahl method, whereas K was measured with a Flame Photometer in accordance with the procedures specified by AOAC (1995). The ascorbic acid content was evaluated using the methods established by Oser (1979), while the total soluble sugars were determined following the procedures of Dubois et al. (1965).

2.2 Experimental Design and Growth Characteristics

The seeds of fenugreek (*Trigonella foenum-graecum* L.) were obtained from the Agricultural Research Center in

Giza, Egypt. Before experimentation, the seeds underwent a surface sterilization process by immersing them in a 5% sodium hypochlorite solution for 5 min. with continuous stirring. Subsequently, the seeds were rinsed multiple times with distilled water. To prime the seeds, they were subjected to either distilled water or an aqueous garlic extract (AGE) at a concentration of 25% (w/v) for a period of 12 h. After priming, the seeds were thoroughly washed with distilled water. Under controlled greenhouse conditions, the primed seeds were planted in plastic pots (20 cm diameter and 15 cm depth) filled with a mixture of clay and sandy soil (2:1 w/w). The greenhouse environment maintained a photoperiod of 10 h with a temperature range of 28/16 ± 2ºC (day/night) and a relative humidity of 60%. Throughout the growth period, the pots were appropriately irrigated with tap water to ensure adequate moisture levels for germination. After 14 days of sowing, both the water-primed and AGE-primed seedlings were further divided into two treatment groups. These treatments involved irrigation with 1000 ml of either distilled water or a sublethal concentration of 50 mM sodium arsenate ($Na_2HAsO_4.7H_2O$), which was determined based on a preliminary experiment, administered directly to the soil surface on the 14th and 18th day of growth. Each treatment group consisted of four pots, arranged in a randomized complete block design. On the 20th day of growth, the seedlings were carefully harvested and subjected to a thorough washing using distilled water. Subsequently, some of the seedlings were promptly used for growth evaluation, while the remaining samples were stored at -80 °C for the subsequent biochemical analyses.

2.3 Assessment of Plant Growth Characteristics

The plant height measurements were obtained from a randomly selected subset of four samples for each treatment group. Immediately after harvesting, the fresh masses (FM) of the seedling's shoots were determined, while the dry masses (DM) were assessed after subjecting the shoot samples to air-forced drying in an oven at 60 °C until a constant weight was achieved. The shoot water content (SWC) was calculated using the formula: $SWC = \left(\frac{FM-DM}{FM}\right) x100$.

Subsequently, the dried samples were thoroughly ground into a 20 mm powder and stored in properly sealed paper bags at 4 °C for subsequent analyses.

2.4 Estimation of Photosynthetic Pigments and Photosynthetic Rate (Fv/FM)

To estimate the levels of chlorophylls and carotenoids, their contents were extracted using 80% acetone following the methods of Arnon (1949) and Horvath et al. (1972), respectively. The pigment contents were expressed as mg/g FM, following measuring the absorbance at 663 nm, 644 nm, and 480 nm using a UV/visible spectrophotometer. The photosynthetic activity of dark-adapted leaves was measured using a digital fluorometer (OS-30 P, Hudson, USA) on the second mature leaf from the stem base.

2.5 Quantification of Osmolytes Level

The total amino acid (TAA) content was determined following the method described by Lee and Takahashi (1966). A 0.1 g sample of dry matter was extracted using 95% ethanol. An aliquot of 0.1 ml of the extract was incubated in a boiling water bath for 15 min. with a mixture of ninhydrin-glycerol-citrate buffer (pH 5.5). The amino acid content was calculated in mg/g DM using glycine as a standard. For free proline (FP) estimation, the plant dry matter was homogenized in 3% aqueous sulfosalicylic acid. The crude extract was boiled with the acid ninhydrin reagent. The resulting chromophore was extracted with toluene, and its absorbance was measured at 520 nm. The proline content was calculated as mg/g DM using a calibration curve generated with proline (Bates et al. 1973). Glycine betaine (GB) was measured according to the method described by Grieve and Grattan (1983). The aqueous extract of the plant dry matter was mixed with 2 N HCl (1:1 v/v) and incubated with cold KI-I2 reagent while constantly stirring. The resulting periodate crystals were extracted with 1,2 dichloroethane, and the absorbance was recorded at 365 nm. A standard curve using glycine betaine was utilized to calculate the glycine betaine content as µg/g DM.

2.6 Determination of Arsenate (As) Content

The content of As in the shoot and root samples was determined in wet digested samples. A mixture of 0.5 g of dry shoot and root samples with 5 ml of HNO_3 and 3 ml of H_2O_2 was used to obtain a clear digestate. The content of As was calculated as µg/g DM using inductively coupled plasma-optical spectroscopy (Polyscan 61 E, Thermo Jarrell-Ash Corp., Franklin, MA, USA).

2.7 Stress Biomarkers Determination

The evaluation of stress biomarkers involved the measurement of hydrogen peroxide (H_2O_2), hydroxyl radical ($OH^{\bullet}$), and malondialdehyde (MDA) contents in fresh leaves. Following the methodology outlined by Velikova et al. (2000), the H_2O_2 content was extracted from fresh leaves using 0.1% trichloroacetic acid (TCA). The extract was then mixed with K-phosphate buffer (pH 7.0) and KI_2 (1 M). The absorbance of the resulting mixture was measured at

390 nm, and the H_2O_2 content was calculated as µM/g FM using a coefficient of 0.28 μM^{-1} cm^{-1}. To assess the $OH^{\bullet}$ content, leaf tissues were extracted in phosphate buffer (pH 7.4) containing 2-deoxyribose (15 mM), following the method of Kaur et al. (2012). The resulting extract (0.7 ml) was subjected to boiling for 30 min. along with a mixture of 0.5% (w/v) thiobarbituric acid (TBA) and glacial acetic acid (3:1 v/v). After cooling, the optical density of the mixture was recorded at 532 nm and 600 nm. The $OH^{\bullet}$ content was expressed as µmol/g FM using an extinction coefficient of 155 mM^{-1} cm^{-1}. For the measurement of lipid peroxidation product (MDA), the samples were homogenized in 5% TCA. The resulting extract was incubated with 0.67% (w/v) thiobarbituric acid (TBA) at 100 °C for 20 mi., followed by immediate cooling. The absorbance was measured at 532 nm and 600 nm, and the extinction coefficient (155 mM^{-1} cm^{-1}) was employed to calculate the MDA content as µmol/g FM (Heath and Packer 1968).

2.8 Estimation of Antioxidant Enzymes

To extract the antioxidant enzymes, fresh leaf samples (0.5 g) were homogenized in pre-chilled K-phosphate buffer (50 mM, pH 7) and centrifuged at 10,000 rpm for 20 min. The resulting enzyme extract was used for measuring the activity of antioxidant enzymes, including catalase (CAT), ascorbate peroxidase (APX), guaiacol peroxidase (GPOX), superoxide dismutase (SOD), polyphenol oxidase (PPO), and glutathione reductase (GR). Superoxide dismutase (SOD) activity was assessed by initiating the photochemical reduction of nitroblue tetrazolium (NBT) using a reaction mixture consisting of the enzyme extract, L-methionine, NBT, Triton X-100, and riboflavin in K-phosphate buffer (pH 7.8). The reaction was initiated by illuminating the mixture for 15 min. and the reduction product of NBT was measured at 560 nm (Beyer and Fridovich 1987). SOD activity was calculated using an extinction coefficient of 21.1 mM^{-1} cm^{-1}. Catalase (CAT) activity was measured by estimating the rate of H_2O_2 decomposition at 240 nm. The enzyme extract was added to a solution of H_2O_2 in K-phosphate buffer (pH 7) and the reduction in absorbance was followed at 240 nm. CAT activity was calculated using an extinction coefficient of 40 mM^{-1} cm^{-1} (Kato and Shimizu 1987). Guaiacol peroxidase (GPOX) activity was assayed by measuring the rate of guaiacol oxidation by H_2O_2. The reaction mixture contained guaiacol (7.2 mM), H2O2 (11.8 m), and enzyme extract in K-phosphate buffer (pH 5.8). The change in absorbance at 470 nm was followed to express GPOX activity using an extinction coefficient of 26.6 mM^{-1} cm^{-1} (Kato and Shimizu 1987).

Ascorbate peroxidase (APX) activity was assessed by measuring the rate of H_2O_2-dependent ASA oxidation. The enzyme extract was added to a reaction mixture containing ASA, H_2O_2, and EDTA in K-phosphate buffer (pH 7). APX activity was calculated at 290 nm using an extinction coefficient of 2.8 mM^{-1} cm^{-1} (Nakano and Asada 1981). Polyphenol oxidase (PPO) activity was evaluated by incubating the enzyme extract with tannic acid in K-phosphate buffer (pH 6.0). After a 5 min. incubation at 25 °C, the reaction was terminated, and the absorbance was recorded at 420 nm. PPO activity was expressed using an extinction coefficient of 26.40 mM^{-1} cm^{-1} (Kumar and Khan 1982). Glutathione reductase (GR) activity was estimated by measuring the oxidative rate of NADPH using oxidized glutathione (GSSG) in a mixture of K-phosphate buffer, EDTA, NADPH, and GSSG. GR activity was calculated by recording the decrease in absorbance at 340 nm using an extinction coefficient of 6.2 mM^{-1} cm^{-1} (Halliwell and Foyer 1978).

2.9 Estimation of Non-Enzymatic Antioxidants

Ascorbic acid (ASA) was extracted from the fresh leaves in 5% aqueous sulfosalicylic acid. Leaf extracts were mixed with Na-molybdate (2%), H_2SO_4 (0.15 N), and Na_2HPO_4 (1.5 mM) (2:2:1 v/v), then incubated at 60 °C for 40 min. The ASA content (mg/g FM) was determined by measuring the absorbance at 660 nm and using a standard curve of ASA (Oser 1979). The reduced glutathione (GSH) was extracted in 5% sulfosalicylic and assessed in fresh leaves as described by Andersen (1985). A 0.5 ml extract was added to the mixture of 100 mM K-phosphate buffer (pH 7), 0.5 mM EDTA, and 3 mM 5,5′-dithiobis (2-nitrobenzoic acid). The absorbance was measured at 412 nm and GSH content (µg/g FM) was assessed with the aid of a GSH calibration curve. The dry leaves of fenugreek were extracted in ethanol to estimate flavonoids and phenolics contents. According to Chang et al. (2002), flavonoids were detected by mixing 0.5 ml extract with a mixture of 10% $AlCl_3$, 1 M K-acetate, and 95% ethanol. After 30 min., the absorbance was recorded at 417 nm using quercetin as a standard flavonoid. According to Jindal and Singh (1975), phenolics were determined by adding 0.1 extract to a mixture of 0.1 ml Folin-Ciocalteu's reagent and 1 ml of 20% Na_2CO_3. After 1 h, the absorbance was measured at 650 nm against standard phenol (gallic acid). The flavonoid and phenolic contents were then reported as mg/ g DM.

2.10 Ultra-Structure Study

For transmission electron microscope (TEM) analysis, the seedling leaves and roots were thoroughly washed with distilled water to remove any residues. Specific leaf sectors and small sections of the main root were then fixed in a 4% aqueous glutaraldehyde solution and subsequently immersed in

a 1% potassium permanganate solution for 5 min at room temperature. The samples were washed three times with distilled water and dehydrated using a series of ethanol solutions. After dehydration, the samples were embedded in an epoxy resin and prepared for sectioning. Ultrathin sections, ranging from 50 to 80 nm in thickness, were mounted on copper grids and stained with uranyl acetate and Reynold's lead citrate (Reynolds 1963). The stained ultrathin sections were examined using a JEOL 1010 transmission electron microscope (JEOL, Peabody, MA).

2.11 Statistical Analysis

The experiment was conducted using a randomized complete block (RCB) design with factorial arrangements. The obtained results were subjected to a one-way ANOVA test using CoStat software (CoHort, V. 6.311) to compare the data means ± standard deviation (SD). To determine the significance of the acquired data, the treatment means were categorized based on the least significant difference (LSD) at a probability level of 0.05. The normality of the data was assessed from the mean and SD values. If the p-value obtained from the statistical test is greater than 0.05, the null hypothesis is accepted, indicating that the data can be considered normally distributed. Additionally, if the standard deviation is less than half of the mean (i.e., less than 50% of the mean), the data are classified as normal (Whitley and Ball 2002). Pearson's correlation coefficients between the investigated traits were used to evaluate the level and type of association between each pair of traits using GraphPad Prism software (version 8.3.0) at a significance level of $P \leq 0.05$.

3 Results

3.1 Phytochemical Constituents of AGE by GC-MS

As evidenced by the results obtained from the GC-MS analysis, the aqueous garlic extract (AGE) exhibited a diverse range of bioactive phytochemical components (Table 1 and Figure S1). Notably, the major phytochemicals identified in the AGE were found to be organosulfur compounds. These compounds included diallyl disulphide, butanethioic acid, S-methyl ester, 1-propene, 3,3'-thiobis-, 3-vinyl-1,2-dithiacyclohex-4-ene, 3-vinyl-1,2-dithiacyclohex-5-ene, 1,3-dithian-2-one, 5,5-dimethyl-, vinyl ethyl sulfoxide, diallyl sulfide, allicin, and 2-myristynoyl pantetheine. The peak area percentages corresponding to these components were determined to be 0.800, 2.015, 0.197, 7.170, 20.167, 0.634, 0.201, 1.116, 8.324, and 0.212%, respectively. Consequently, it can be inferred that 3-vinyl-1,2-dithiacyclohex-4-ene, allicin, and 3-vinyl-1,2-dithiacyclohex-5-ene were the primary organosulfur compounds present in the AGE. Furthermore, the analysis revealed the presence of other non-sulfurous phytocomponents in the extract, which exhibited relatively high area percentages. These components included DL-3-phenyllactic acid, 2-hydroxyoctanoic acid, butylated hydroxytoluene, phthalic acid, butyl isohexyl ester, and 1,2-benzenedicarboxylic acid, diisooctyl ester, with peak area percentages of 1.398, 3.602, 3.076, 2.390, and 8.979%, respectively. It is worth mentioning that the AGE also contained other significant active phytochemicals with varying area percentages. These findings highlight the complex composition of the extract and suggest its potential as a source of diverse bioactive compounds.

3.2 Chemical Composition of AGE

The chemical composition of the AGE, as illustrated in Table 2, exhibited a diverse array of biologically active compounds. AGE demonstrated significant levels of soluble sugars and ascorbic acid (143.25 and 35.05 µg/ml, respectively). Additionally, it contained notable concentrations of phytohormones such as gibberellic acid, abscisic acid, indole 3-acetic acid, and cytokinins (3.74, 0.45, 0.20, and 0.27 µg/ml, respectively). Moreover, it was observed to encompass a spectrum of macronutrients including phosphorus, nitrogen, sulfur, calcium, magnesium, and potassium (115.01, 0.81, 0.29, 0.54, 0.20, and 1.15 µg/ml, respectively). Similarly, AGE displayed significant levels of the micronutrients analyzed, including selenium, zinc, copper, iron, manganese, and molybdenum (0.271, 0.084, 0.012, 0.015, 0.151, and 0.003, respectively).

3.3 Growth Patterns

The impact of arsenate (As) stress on the growth characteristics of fenugreek seedlings is presented in Table 3. Exposure to As stress led to a significant reduction in the growth parameters of the seedlings, including plant height, fresh mass, and dry mass, which decreased by 25.0, 47.6, and 32.1%, respectively, compared to the control treatment. Additionally, a decrease of 3.1% in shoot water content (SWC) was observed in As-stressed seedlings relative to the control. However, when the seeds were primed with AGE, a notable improvement in the growth traits of As-stressed fenugreek seedlings was observed. The priming treatment with AGE resulted in a significant increase of 29.2, 31.8, and 32.1% in shoot height, fresh mass, and dry mass, respectively, compared to the As-stressed treatment. Furthermore, the priming with AGE led to a relative improvement of 1.1% in SWC compared to As-stressed fenugreek seedlings. It is worth noting that under non-stress conditions, the priming

Table 1 GC-MS analysis of the phytochemically active constituents in the Garlic bulb aqueous extract

Pk #	RT (min)	Compound Name	Area %	Molecular formula	Class
1	6.424	Benzyl alcohol	0.519	C_7H_8O	Aromatic alcohol
2	7.314	3,4-dihydroxy-4-methylpentan-2-one	0.388	$C_6H_{12}O_3$	Keton derivative
3	7.844	Benzaldehyde, 3-methyl-	0.304	C_8H_8O	Benzoyl derivative
4	8.234	2,4-Hexadienoic acid, ethyl ester	0.317	$C_8H_{12}O_2$	Organic acid
5	8.394	Diallyl disulphide	0.800	$C_6H_{10}S_2$	Organosulfur
6	9.235	Butanethioic acid, S-methyl ester	2.015	$C_5H_{10}OS$	Organosulfur
7	9.410	L-2-Aminobutyric acid	0.574	$C_4H_9NO_2$	Amino acid
8	9.435	Phenylacetic acid, 2-dimethylaminoethyl ester	0.804	$C_{12}H_{17}NO_2$	Amino derivative
9	10.500	(R)-3-Hydroxybutyric acid	0.589	$C_4H_8O_3$	Fatty acid
10	10.710	3-Methyl-2-butenoic acid, phenyl ester	0.195	$C_{13}H_{16}O_2$	Carboxylic acid
11	11.295	1-Propene, 3,3'-thiobis-	0.197	$C_6H_{10}S$	Organosulfur
12	11.375	DL-3-Phenyllactic acid	1.398	$C_9H_{10}O_3$	Carboxylic acid
13	11.741	Propanamide, 2-methyl-	0.337	C_4H_9NO	Amide derivative
14	11.891	3-Vinyl-1,2-dithiacyclohex-4-ene	7.170	$C_6H_8S_2$	Organosulfur
15	12.326	3-Hexanol, 2,4-dimethyl-	0.646	$C_8H_{18}O$	Organic alcohol
16	12.506	3-Vinyl-1,2-dithiacyclohex-5-ene	20.167	$C_6H_8S_2$	Organosulfur
17	12.761	2-Furancarboxaldehyde, 5-(hydroxymethyl)-	0.412	$C_6H_6O_3$	Aryl aldehyde
18	13.291	2,2'-Bi-1,3-dioxolane	0.275	$C_6H_{10}O_4$	Heterocyclic acetal
19	13.576	Nonanoic acid	0.247	$C_9H_{18}O_2$	Fatty acid
20	13.957	1,3-Dithian-2-one, 5,5-dimethyl-	0.634	$C_6H_{10}OS_2$	Organosulfur
21	14.277	2-Hydroxyoctanoic acid	3.602	$C_8H_{16}O_3$	Fatty acid
22	14.412	Vinyl ethyl sulfoxide	0.201	C_4H_8OS	Organosulfur
23	15.112	Diallyl sulfide	1.116	$C_6H_{10}S$	Organosulfur
24	15.612	2-Methyl-n-1-tridecene	0.642	$C_{14}H_{28}$	Acyclic olefin
25	17.048	Allicin	8.324	$C_6H_{10}OS_2$	Organosulfur
26	17.248	Butylated hydroxytoluene	3.076	$C_{15}H_{24}O$	Phenolic compound
27	17.483	Octanoic acid, 7-oxo-	0.737	$C_8H_{14}O_3$	Fatty acid
28	17.558	2-Myristynoyl pantetheine	0.212	$C_{25}H_{44}N_2O_5S$	Organosulfur
29	17.798	Scyllo-Inositol	0.652	$C_6H_{12}O_6$	Sugar alcohol
30	17.893	Tetratetracontane	0.210	$C_{44}H_{90}$	Alkane
31	21.500	3-Isopropyl-4-methyl-dec-1-en-4-ol	0.227	$C_{14}H_{28}O$	Alcohol derivative
32	21.790	5-Octadecene, (E)-	0.252	$C_{18}H_{36}$	Hydrocarbon
33	24.326	Phthalic acid, butyl isohexyl ester	1.036	$C_{18}H_{26}O_4$	Aromatic acid
34	24.386	n-Hexadecanoic acid	2.390	$C_{16}H_{32}O_2$	Fatty acid
35	27.342	1,11-Dodecadiene	1.118	$C_{12}H_{22}$	Hydrocarbon
36	27.442	8-Hexadecenal, 14-methyl-, (Z)-	0.346	$C_{17}H_{32}O$	Aliphatic aldehyde
37	27.882	Octadecanoic acid	0.436	$C_{18}H_{36}O_2$	Fatty acid
38	30.348	Heptane, 2,2,3,3,5,6,6-heptamethyl-	0.222	$C_{14}H_{30}$	Alkane
39	33.609	Octadecane, 1-(ethenyloxy)-	0.227	$C_{20}H_{40}O$	Alkane
40	33.749	1,2-Benzenedicarboxylic acid, dicyclohexyl ester	0.657	$C_{20}H_{26}O_4$	Carboxylic acid
41	33.850	2-Nonanol	0.336	$C_9H_{20}O$	Fatty alcohol
42	34.220	1,2-Benzenedicarboxylic acid, diisooctyl ester	8.979	$C_{24}H_{38}O_4$	Carboxylic acid
43	35.180	Sinapic acid	0.262	$C_{11}H_{12}O_5$	Phenylpropanoid
44	36.911	2,4,6-Cycloheptatrien-1-one, 3,5-bis-trimethylsilyl	0.509	$C_{13}H_{22}OSi_2$	Organosilicon derivative

Table 2 The chemical composition of the aqueous Garlic extract (AGE)

Phytocomponents of AGE (µg/ml extract)			
Soluble sugars	143.25	Ascorbic acid	38.05
Phytohormones			
Gibberellic acid	3.74	Abscisic acid	0.45
Indole 3-acetic acid	0.20	Cytokinins	0.27
Mineral composition			
Phosphorus	115.01	Selenium	0.271
Nitrogen	0.81	Zinc	0.084
Sulfur	0.29	Cupper	0.012
Calcium	0.54	Iron	0.015
Magnesium	0.20	Manganese	0.151
Potassium	1.51	Molybdenum	0.003

Table 3 Effect of seed priming with aqueous Garlic extract (AGE) on growth parameters of sodium arsenate-irrigated Fenugreek seedlings

Treatments	**Shoot height (cm)**	**FM (g/plant)**	**DM (g/plant)**	**SWC (%)**
Control	18.38 ± 1.66^{b}	0.42 ± 0.03^{a}	0.028 ± 0.002^{a}	93.3 ± 0.78^{a}
AGE	22.58 ± 1.49^{a}	0.38 ± 0.06^{a}	0.033 ± 0.006^{a}	93.2 ± 1.33^{a}
As	13.78 ± 0.46^{c}	0.22 ± 0.01^{c}	0.019 ± 0.002^{b}	90.4 ± 0.32^{b}
AGE + As	17.80 ± 1.16^{b}	0.29 ± 0.02^{b}	0.028 ± 0.002^{a}	91.4 ± 0.29^{b}
Source of variation				
F	31.71	29.60	11.42	18.65
P	0.0000	0.0000	0.0008	0.0001
LSD at 0.05	2.760	0.070	0.007	1.401

FM = Fresh mass; DM = Dry mass; SWC = Shoot water content. Significant differences were highlighted by different letters in the same column at $P \leq 0.05$

with AGE had a somewhat positive impact on the growth attributes of fenugreek when compared to the untreated control treatment.

3.4 Photosynthetic Parameters

The data in Table 4 illustrate the impact of As exposure on the photosynthetic activity and pigment content of fenugreek leaves. Arsenate exposure led to a significant reduction in photosynthetic activity (Fv/Fm), with a decrease of 9.0% compared to the untreated control. Moreover, the stressed seedlings exhibited a substantial decline in both Chl a and Chl b levels, with decreases of 66.3, and 67.1%, respectively, relative to the control. In contrast, the carotenoid content of fenugreek leaves showed a significant increase of 9.2% following the As application compared to the control. Interestingly, priming the As-stressed fenugreek seedlings with AGE significantly enhanced photosynthetic parameters. Pre-soaking in AGE restored the photosynthetic activity to the same level as the untreated control. Furthermore, priming with AGE significantly increased chlorophyll levels beyond those of the control treatment and mitigated the declines in Chl a and Chl b caused by As stress, with increases of 337.5 and 342.5%, respectively. The As-induced increase in carotenoid content was significantly reduced by AGE application, resulting in a decrease of 35.6% compared to the As stress treatment. Moreover, when fenugreek seedlings were treated with AGE alone, a non-significant decline in the Fv/Fm was observed, indicating a marginal effect on the photosynthetic efficiency. However, carotenoid content showed a substantial decrease of 59.8% relative to the control. On the other hand, Chl a and Chl b levels exhibited a significant enhancement of 77.9 and 72.2%, respectively, compared to the control. These findings highlight the beneficial effects of AGE priming in mitigating the adverse effects of As stress on the photosynthetic activity and pigment content of fenugreek leaves.

3.5 Osmolytes Content

The data presented in Table 5 demonstrate the influence of As and AGE treatments on the concentration of osmolytes in fenugreek leaves. Regarding osmoregulation, exposure to As stress significantly elevated the levels of total amino acids (TAA), free proline (FP), and glycine betaine (GB) in fenugreek seedlings. This treatment resulted in increases of 25.6, 155.8, and 5.5% in TAA, FP, and GB, respectively, compared to the untreated control. However, priming As-stressed fenugreek seedlings with AGE led to an overproduction of these osmoregulators. The priming treatment resulted in increases of 9.7, 5.0, and 31.8% in the accumulation ratios of TAA, FP, and GB, respectively. Furthermore, AGE-treated fenugreek seedlings exhibited an increased

Table 4 Effect of seed priming with aqueous Garlic extract (AGE) on photosynthetic rate (Fv/Fm) and pigments of sodium arsenate-irrigated Fenugreek seedlings

Treatments	**Fv/Fm**	**Photosynthetic pigments (mg/g FM)**		
		Chl a	**Chl b**	**Carotenoids**
Control	0.78 ± 0.010^{a}	9.5 ± 0.035^{c}	5.44 ± 0.320^{c}	3.68 ± 0.025^{b}
AGE	0.77 ± 0.006^{ab}	16.9 ± 0.055^{a}	9.37 ± 0.470^{a}	1.48 ± 0.025^{d}
As	0.71 ± 0.020^{b}	3.2 ± 0.055^{d}	1.79 ± 0.006^{d}	4.02 ± 0.030^{a}
AGE + As	0.78 ± 0.005^{a}	14.0 ± 0.210^{b}	7.92 ± 0.005^{b}	2.59 ± 0.028^{c}
Source of variation				
F	9.20	8682.48	382.86	5402.86
P	0.0057	0.0000	0.0000	0.0000
LSD at 0.05	0.032	0.312	0.778	0.074

Significant differences were highlighted by different letters in the same column at $P \leq 0.05$

Table 5 Effect of seed priming with aqueous Garlic extract (AGE) on osmolytes content of sodium arsenate-irrigated Fenugreek seedlings

Treatments	TAA (mg/g DM)	FP (mg/g DM)	GB (µg/g DM)
Control	49.94 ± 6.8^{b}	10.57 ± 0.5^{b}	1.46 ± 0.06^{c}
AGE	61.33 ± 0.2^{a}	10.02 ± 0.5^{b}	1.62 ± 0.01^{b}
As	62.72 ± 0.4^{a}	27.04 ± 0.02^{a}	1.54 ± 0.01^{bc}
AGE + As	68.83 ± 0.9^{a}	28.39 ± 0.9^{a}	2.03 ± 0.09^{a}
Source of variation			
F	15.80	925.61	64.44
P	0.0010	0.0000	0.0000
LSD at 0.05	9.401	1.570	0.150

TAA = Total amino acids; FP = Free proline; GB = Glycine betaine. Significant differences were highlighted by different letters in the same column at $P \leq 0.05$

Table 6 Effect of seed priming with aqueous Garlic extract (AGE) on arsenate contents of sodium arsenate-irrigated Fenugreek seedlings

Treatments	Arsenate (µg/g DM)	
	Root	Shoot
Control	0.085 ± 0.001^{c}	0.032 ± 0.001^{b}
AGE	0.051 ± 0.002^{c}	0.017 ± 0.002^{b}
As	7.295 ± 0.005^{a}	6.053 ± 0.015^{a}
AGE + As	3.737 ± 0.024^{b}	1.259 ± 0.064^{b}
Source of variation		
F	18090.01	23.34
P	0.0000	0.0000
LSD at 0.05	0.084	1.620

Significant differences were highlighted by different letters in the same column at $P \leq 0.05$

accumulation of the osmoprotectant molecules TAA and GB (22.8 and 11.0%, respectively), while the accumulation of FP decreased by 5.2% compared to the untreated control.

3.6 Arsenate Content

Table 6 provides an insight into the levels of arsenate (As) in the shoot and root systems of fenugreek plants in response to As and AGE treatments. The findings demonstrated that seedlings exposed to As accumulated higher levels of As in both their roots and shoots, with concentrations of 7.295 and 6.053 µg/g DM, respectively, compared to the control treatment (0.085and 0.032 µg/g DM, respectively). Notably, the root system exhibited the highest content of As accumulation. In comparison to the single As-stressed treatment, priming with AGE in combination with As stress resulted in significantly reduced As accumulation in both the root and shoot systems, with concentrations of 3.737 and 1.259 µg/g DM, respectively. Moreover, when AGE was applied as a single treatment, it showed the lowest levels of As in the root and shoot systems of fenugreek, with concentrations of 0.051 and 0.017 µg/g DM, respectively.

3.7 Oxidative Stress Biomarkers

The data presented in Fig. 1 provide insights into the response of fenugreek seedlings to As stress and the application of AGE as a priming agent. The results demonstrate a substantial increase in oxidative stress biomarkers, including H_2O_2, $OH^{\bullet}$, and MDA contents (Fig. 1A and B, and 1C, respectively), by 47.3, 60.8, and 146.2%, respectively, in response to As stress compared to the control. Conversely, priming with AGE effectively mitigated these oxidative events, resulting in a significant reduction in H_2O_2, $OH^{\bullet}$, and MDA contents by 48.7, 29.6, and 40.3%, respectively, in comparison to As-stressed seedlings. However, when AGE was applied alone, it exhibited a similar effect to that of the control treatment on oxidative stress biomarkers, except for a slight increase in MDA level.

3.8 Antioxidant Enzymes Activity

The alteration in the activity of antioxidant enzymes in response to experimental treatments is depicted in Fig. 2. The findings indicated that As irrigation led to an increase in the activities of catalase (CAT) (Fig. 2B), guaiacol peroxidase (GPOX) (Fig. 2C), glutathione reductase (GR) (Fig. 2E), and polyphenol oxidase (PPO) (Fig. 2F) by 7.6, 16.2, 13.9, and 14.2%, respectively, compared to the control treatment. In contrast, superoxide dismutase (SOD) (Fig. 2A) and ascorbate peroxidase (APOX) (Fig. 2D) activities exhibited a significant decline of 72.0 and 31.8%, respectively, in response to As stress compared to the control. Notably, AGE priming resulted in additional increases in GPOX and GR activities by 13.5 and 34.1%, respectively, relative to the As treatment. Moreover, AGE priming effectively restored the activities of CAT and PPO to levels comparable to the control treatment in the presence of As stress. Furthermore, AGE priming caused a pronounced up-regulation in SOD and APOX activities by 599.7 and 33.9%, respectively, compared to the As-stressed treatment. However, when fenugreek seedlings were subjected to AGE treatment alone, a slight decrease in the activities of SOD, GPOX, APOX, and PPO, along with a slight increase in GR and CAT activities, was observed.

3.9 Antioxidant Molecules

Regarding non-enzymatic antioxidant molecules, Fig. 3 illustrates the levels of ascorbic acid (ASA), glutathione (GSH), flavonoids, and phenolic compounds in response to As stress and AGE treatment. The results showed a significant elevation in the levels of ASA, GSH, flavonoids, and phenolic compounds (Fig. 3A, B and C, and 3D, respectively) by 77.3, 28.9, 57.1, and 11.8%, respectively,

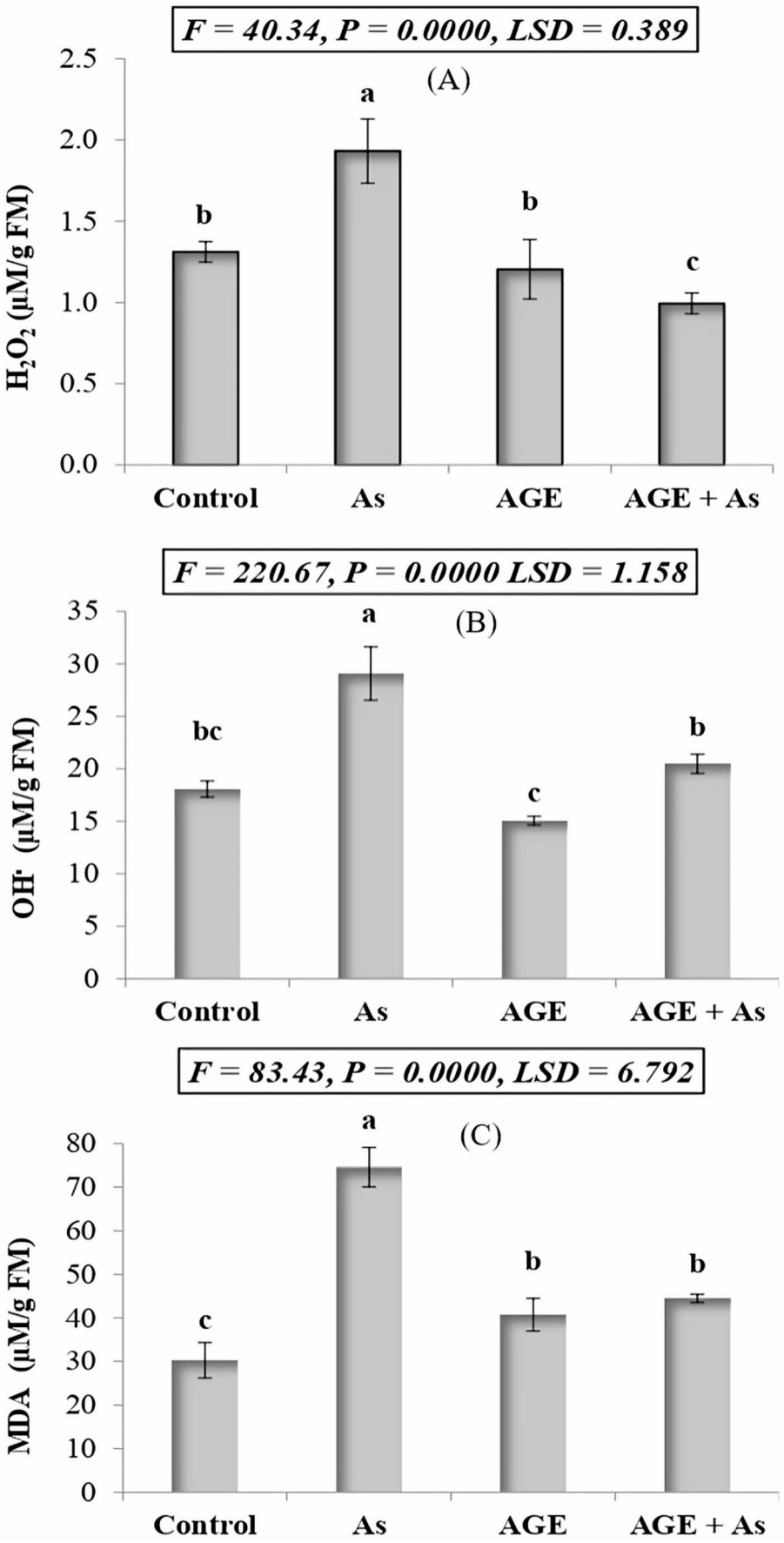


Fig. 1 Effect of seed priming with aqueous garlic extract (AGE) on oxidative stress biomarkers of sodium arsenate-irrigated fenugreek seedlings. (**A**) H_2O_2 = Hydrogen peroxide; (**B**) $OH^{\bullet}$ = Hydroxyl radical; (**C**) MDA = Malondialdehyde. Significant differences were highlighted by different letters at $P \leq 0.05$

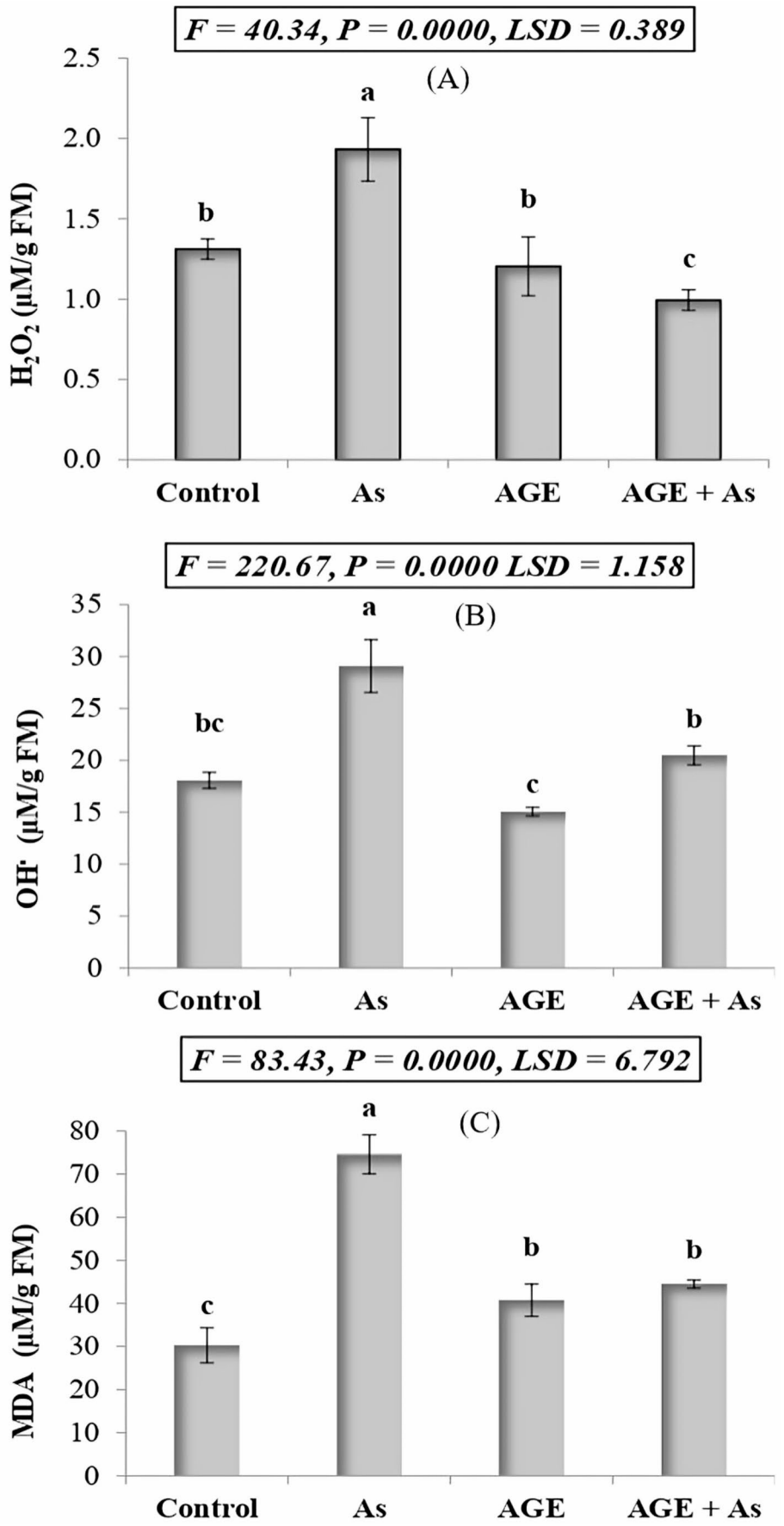


Fig. 2 Effect of seed priming with aqueous garlic extract on (AGE) antioxidant enzymes of sodium arsenate-irrigated fenugreek seedlings. (**A**) SOD = Superoxide dismutase; (**B**) CAT = Catalase; (**C**) GPX = Guaiacol peroxidase; (**D**) APOX = Ascorbate peroxidase; (**E**) GR = Glutathione reductase; (**F**) PPO = Polyphenol oxidase. Significant differences were highlighted by different letters at $P \leq 0.05$

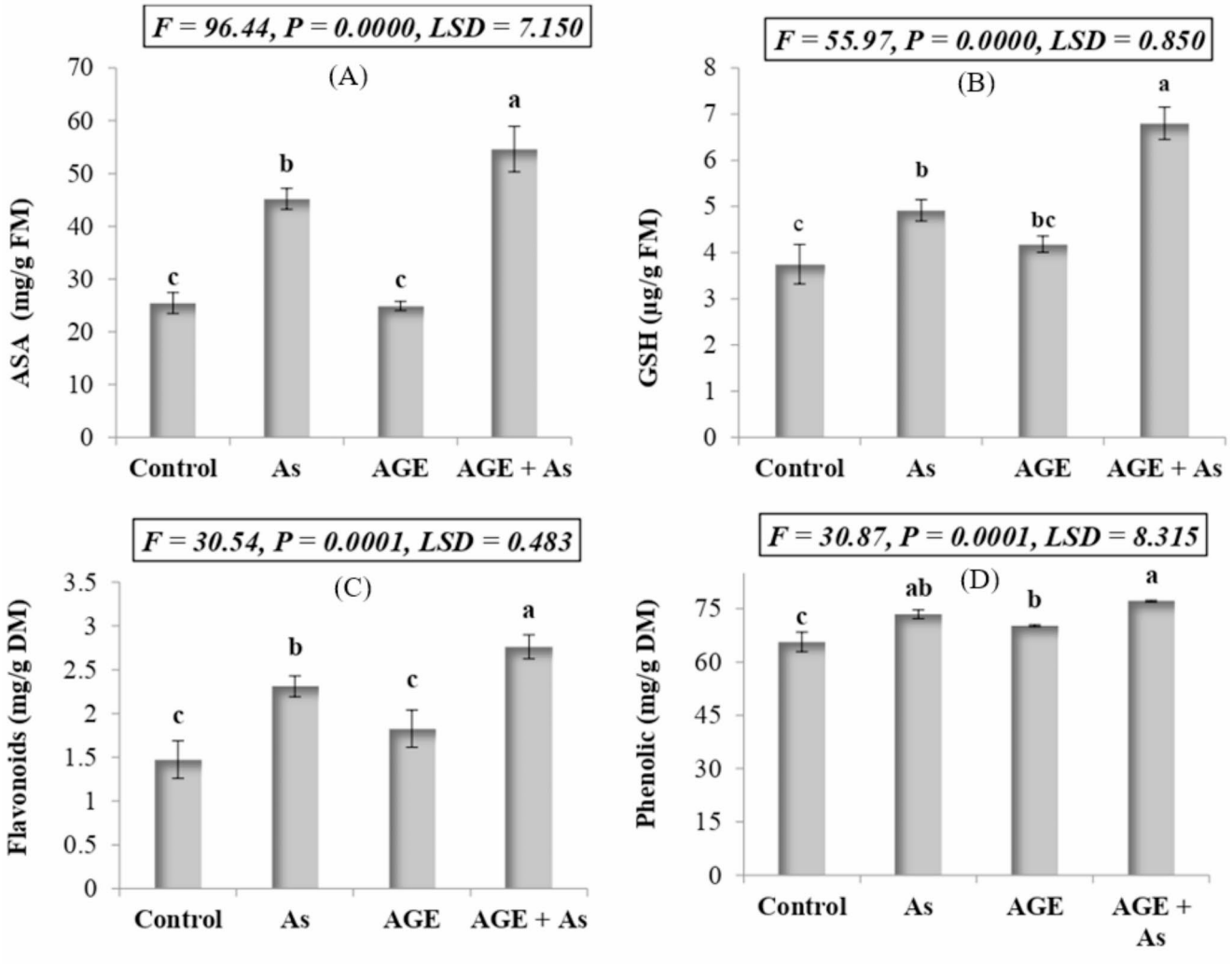


Fig. 3 Effect of seed priming with aqueous garlic extract (AGE) on antioxidant compounds of sodium arsenate-irrigated fenugreek seedlings. (**A**) ASA=Ascorbic acid; (**B**) GSH=Reduced glutathione; (**C**) Flavonoids; (**D**) Phenolics. Significant differences were highlighted by different letters at $P \leq 0.05$

compared to the control treatment. Interestingly, when As-stressed seedlings were treated with AGE as a presoaking treatment, there was a further increase in the contents of ASA, GSH, flavonoids, and phenolics by 20.8, 38.8, 19.5, and 5.0%, respectively, compared to the As stress treatment. However, when fenugreek seedlings were subjected to AGE treatment alone, there was no significant effect on the evaluated antioxidant metabolites, except for a slight decrease in ASA level and a slight increase in GSH, flavonoid, and phenolic compound levels compared to the control treatment.

3.10 Alterations in the Ultrastructure

The transmission electron microscopy (TEM) micrographs presented in Figs. 4 and 5 provide detailed insights into the structural changes observed in leaves and roots, respectively, following the experimental treatments.

3.10.1 Leaf Photographs

In the investigation of leaf sections (Fig. 4), the control samples exhibited intact mesophyll cells with a prominent central vacuole and well-arranged chloroplasts along the cell wall (Fig. 4A). The chloroplasts in the control leaves contained numerous starch grains distributed throughout (Fig. 4B) and exhibited a regular arrangement of grana and well-organized thylakoid membranes (Fig. 4C and D). Conversely, leaf cells exposed to As stress displayed a flaccid appearance (Fig. 4E and F), along with altered chloroplasts characterized by a reduced number of starch grains and severe ultrastructural abnormalities. The toxic effects of As were evident from the presence of cytoplasmic microvesicles (white arrows), accompanied by vesiculation of the plasma membrane (Fig. 4E and F, and 4G) and plasmolysis (Fig. 4F). The swollen chloroplasts, under As-induced stress,

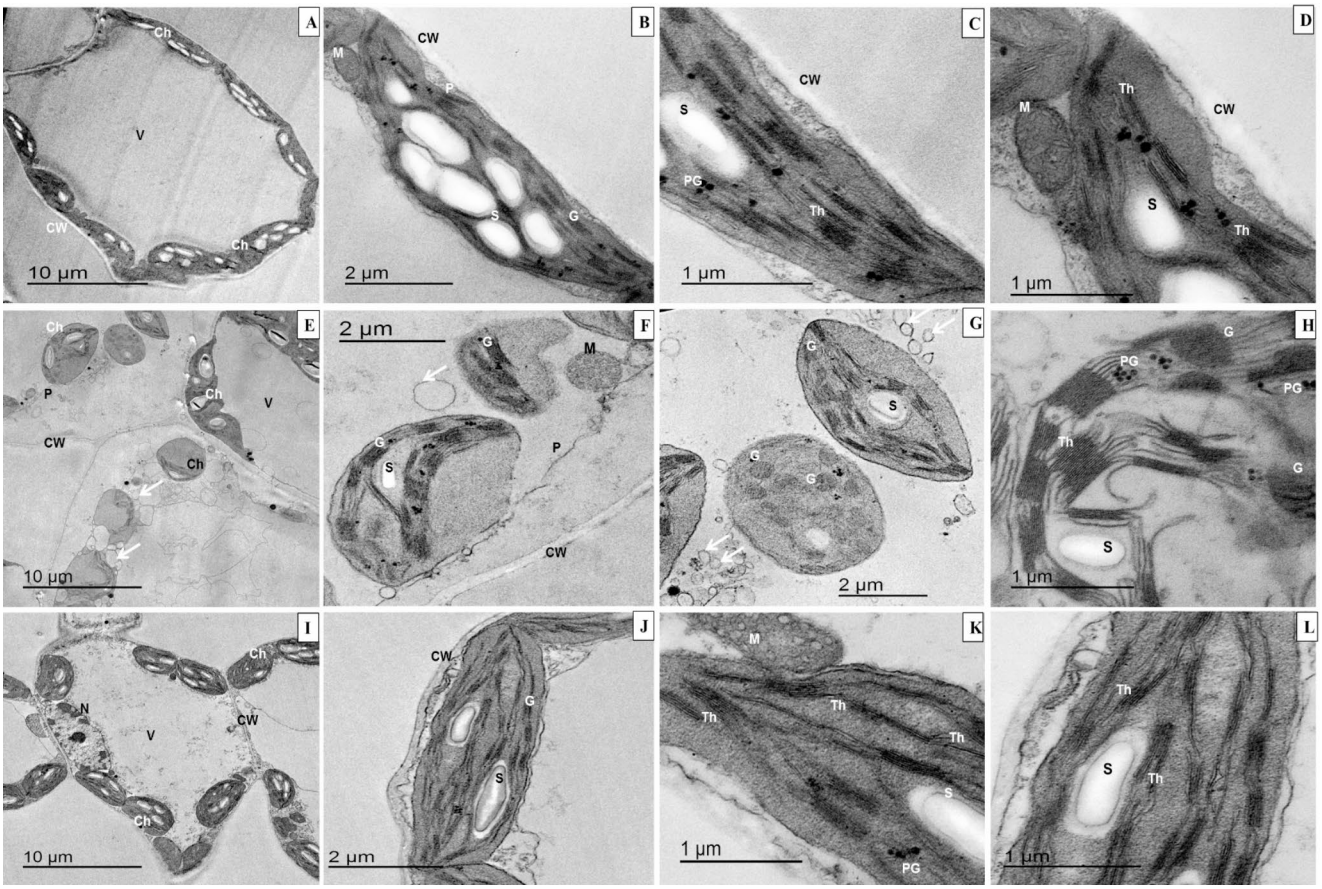


Fig. 4 Transmission electron micrographs of leaf cells of sodium arsenate-irrigated fenugreek seedlings treated with aqueous garlic extract (AGE). (**A-D**) control, (**E-H**) As stress, (**I-L**) combined treatment of As stress and AGE. CW: cell wall, V: vacuole, Ch: chloroplast, G: grana, Th: thylakoids, S: starch, PG: plastoglobuli, N: nucleus, and M: mitochondria

exhibited abnormal globular shapes and disrupted outer membrane structures (Fig. 4E and F, and 4G), with varying degrees of shrinkage in their internal contents, resulting in an expanded chloroplast matrix (Fig. 4F and G). Moreover, As toxicity significantly disrupted thylakoid membranes, leading to the appearance of dark electron-dense plastoglobuli (Fig. 4G and H). The mitochondrial cristae were also adversely affected by As toxicity, exhibiting slight disintegration within a swollen morphology (Fig. 4F). However, priming with AGE substantially alleviated As-induced cellular toxicity. The leaves of seedlings treated with AGE exhibited a predominantly normal chloroplast shape, with intact thylakoid membranes (Fig. 4I and J, and 4K). AGE priming preserved cell turgidity and eliminated plasmolysis (Fig. 4I). Furthermore, the mitochondria regained their well-defined cristae, comparable to those observed in the single As treatment (Fig. 4K).

3.10.2 Roots Photographs

Moving on to root sections (Fig. 5), the control samples displayed xylem vessels with normal construction and thick lignified walls (Fig. 5A), along with intact cell walls (Fig. 5B and C, and 5D). However, the application of As stress resulted in distorted lignification of xylem vessels, characterized by wall breaks (Fig. 5E). As exposure also led to the disintegration of the nucleus, with disrupted chromatin structure (Fig. 5F), in contrast to the unstressed treatment. Additionally, the cell wall exhibited structural events as a consequence of As toxicity, such as noticeable thinning (Fig. 5F and G), detachment from the protoplasm (Fig. 5F), and the appearance of nicks or amoeboid protrusions (Fig. 5H). Moreover, the intercellular spaces appeared blocked, with the accumulation of dark, dense vesicles in response to As treatment (Fig. 5G), potentially indicative of As depositions. However, AGE priming facilitated the restoration of normal cellular structures in the roots. The xylem vessels exhibited normal lignification without any breaks, in contrast to the As-stressed condition (Fig. 5I). Furthermore, priming with AGE enabled the root cells to regain their normal cellular compartments, including the cell wall and nucleus (Fig. 5J and K). However, the intercellular spaces displayed slightly dense As depositions (Fig. 5J and K) when compared to the root cells treated solely with As.

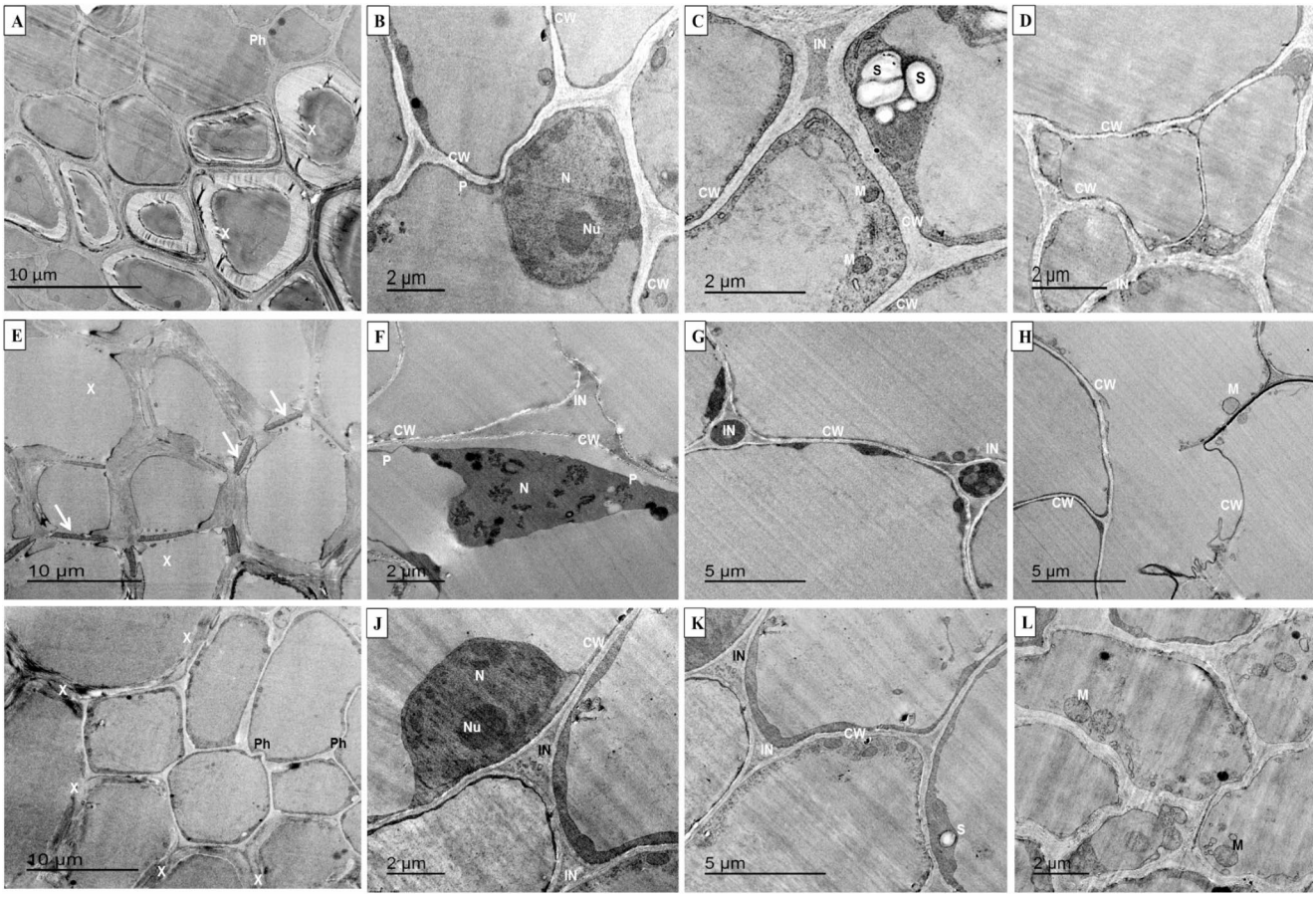


Fig. 5 Transmission electron micrographs of root cells of sodium arsenate-irrigated fenugreek seedlings treated with aqueous garlic extract (AGE). (**A**-**D**) control, (**E**-**H**) As stress, (**I**-**L**) combined treatment of As stress and AGE. X: xylem vessel, Ph: phloem, CW: cell wall, P: plasma membrane, IN: intercellular spaces, S: starch, N: nucleus, and M: mitochondria

3.11 The Correlation Between the Investigated Morpho-Physio-Biochemical Traits

The correlation between the studied morpho-physio-biochemical traits of fenugreek seedlings was assessed through a correlation matrix heatmap, revealing significant positive and negative relationships (Fig. 6). A robust positive correlation was observed between chlorophyll a (Chl a) and chlorophyll b (Chl b), indicating a concurrent increase in Chl b with increasing Chl a level. Similarly, a positive correlation was noted between shoot water content (SWC) and the plant fresh mass (FM), indicating a beneficial impact of increased water availability on plant vigor. Conversely, a notably strong negative correlation was identified between carotenoids (Caro) content and Chl a and Chl b levels, signifying an inverse association where elevated carotenoid concentrations coincide with decreased chlorophyll levels. Moreover, a significant negative correlation was found between root arsenate content (As R) and FM, underscoring a detrimental effect of elevated As R levels on plant health. Interestingly, hydrogen peroxide (H_2O_2) content exhibited a negative correlation with Chl a level, implying an association between elevated H_2O_2 levels and reduced Chl a concentrations indicative of oxidative stress impacting photosynthetic efficiency. Additionally, malondialdehyde (MDA) and catalase (CAT) activities displayed a negative correlation, hinting at compromised CAT function under oxidative stress conditions, potentially affecting the plant's oxidative damage management. Some parameters like superoxide dismutase (SOD) and glutathione (GSH) showed complex relationships with other variables, implying intricate interactions in oxidative stress responses and antioxidant mechanisms. Notably, a generally positive correlation was observed between flavonoid (Flav) levels and various parameters, suggesting a potential role of flavonoids in bolstering plant resilience against heavy metals toxicity.

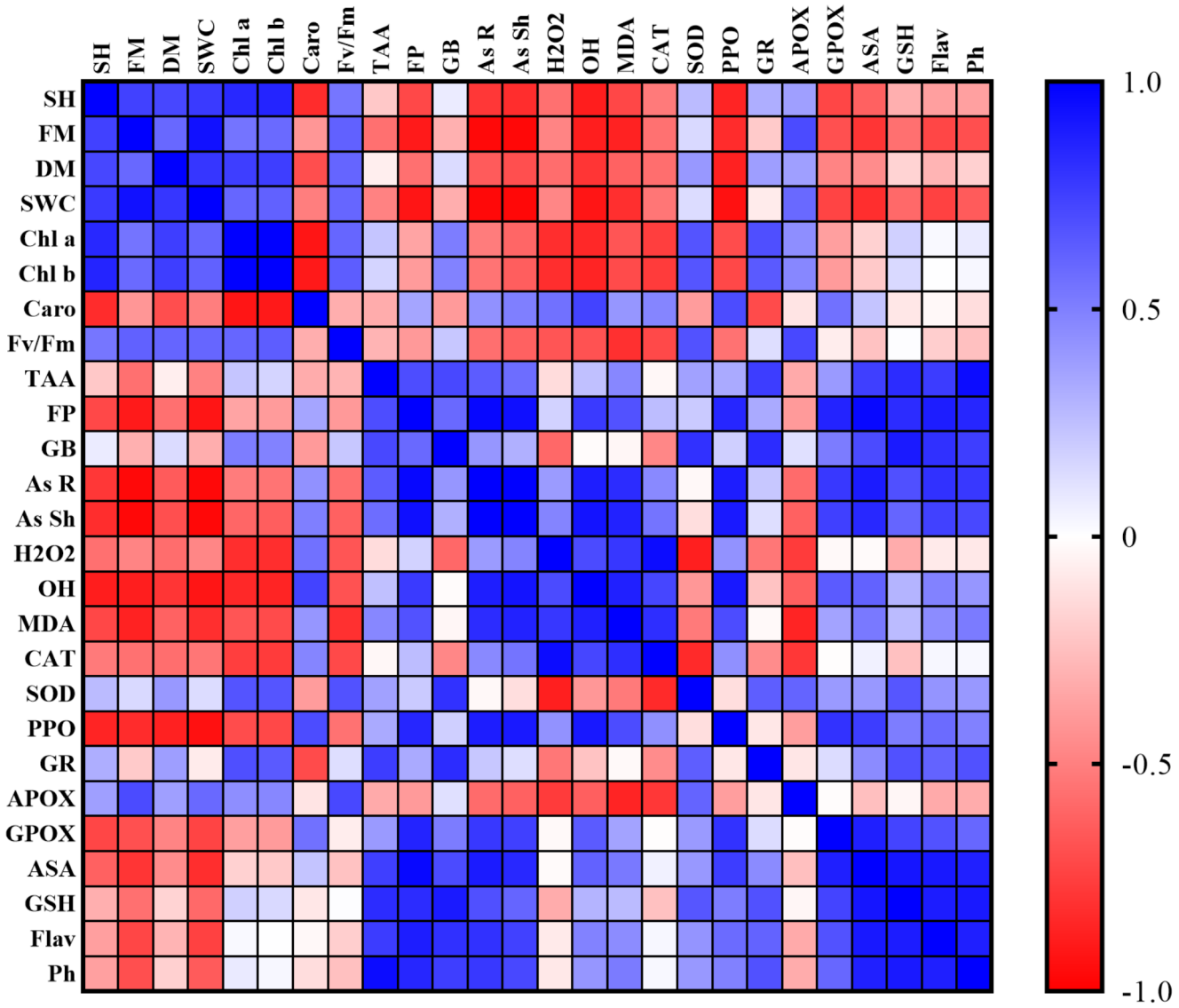


Fig. 6 Parson's correlation matrix heatmap showing the relationship between the investigated parameters in sodium arsenate-irrigated fenugreek seedlings treated with aqueous garlic extract (AGE).SH: shoot height, FM: fresh mass, DM: dry mass, SWC: shoot water content, Chl a: chlorophyll a, Chl b: chlorophyll b, Caro: carotenoids, Fv/Fm: photosynthetic activity, TAA: total amino acids, FP: free proline, GB: glycine betaine, As R: arsenate in root, As S: arsenate in shoot, H_2O_2: hydrogen peroxide, OH: hydroxyl radical, MDA: malondialdehyde, CAT: catalase, SOD: superoxide dismutase, PPO: polyphenol oxidase, GR: glutathione reductase, APOX: ascorbate peroxidase, GPOX: guaiacol peroxidase, ASA: ascorbic acid, GSH: reduced glutathione, Flav: flavonoids, and Ph: phenolics

4 Discussion

Because of the use of fertilizers, metallo-pesticides or herbicides, sewage sludge, and wastewater irrigation, food crops are overexposed to toxic metallic contaminants (Rai et al. 2023). The present investigation demonstrated an overall decrease in the growth of fenugreek seedlings due to As-stress, as indicated by decreases in plant height and biomasses. The inhibition of cellular turgor, cell elongation, and mitotic activity is caused by the increased uptake of As, which interferes with different metabolic activities (Du et al. 2017). Relative to the control, the decreased water content was correlated to the elevated As contents and higher accumulating activity of fenugreek roots. Furthermore, the reduction in moisture content and the decline in water use efficiency, along with the consequential alterations in the structural integrity of the cell wall and the permeability of the plasma membrane, collectively contribute to the impeded growth of plants.

The seed priming with AGE limited the suppression of growth traits induced by As stress with maximum enhancement of dry masses which lightened its protective and stimulating capacity. The enhanced plant tolerance could be elucidated by the high availability of plant

growth-enhancing bioactive chemicals such as phytohormones, amino acids, and nutrients (Zulfiqar et al. 2020). The phytochemical analysis of AGE showed its richness of organic sulfur compounds and phenol-containing phytochemicals, which are known for high antioxidant effects The considerable antioxidant capacity exhibited by AGE holds significant potential to provide substantial protection to fenugreek seedlings cultivated in As-polluted soils. This protection could be achieved due to the potential of AGE to sustain the stability of cellular membranes and organelles, offer protection to the dividing meristems, and increase the turgor pressure of stressed plants. In this context, the application of AGE significantly enhanced the growth pattern of soybean water-stressed plants (Mohamed and Akladious 2014). Thus, enhanced growth could be attributed to the intricate nutritional composition found in the AGE.

The current findings demonstrated that exposure to As stress resulted in an impairment in the photosynthesis process, as evidenced by the depletion of chlorophyll and retardation of photosynthetic activity as a sign of ultrastructural distortions of the chloroplast. A significant decline in Chl a and Chl b levels was recorded by As stress which could be ascribed to their inhibited synthesis and As toxic impacts on bio-membranes, stomatal conductance, and plant mineral nutrition (Abbas et al. 2018). Alternatively, As stress resulted in a significant elevation in carotenoids content over the control. Plants are known to accumulate considerable levels of non-enzymatic antioxidants including carotenoids as a detoxification response to As-induced oxidative toxicity. In photosynthetic systems, carotenoids can relieve photooxidative damage of chlorophyll, scavenge oxidative radicals, and stabilize cellular membranes (Saad-Allah and Ragab 2020). However, the intensive increase in carotenoids level is still inadequately effective in restricting ROS-induced lipid peroxidation of chloroplast membranes as manifested by ultrastructural detections.

The restoration of photosynthetic pigments level was observed due to AGE priming, indicating an improvement in plant performance under As stress. The priming with AGE significantly enhanced photosynthetic activity and increased the levels of Chl a and Chl b, as compared to the treatment with As alone. The reduction of stress-induced symptoms in photosynthetic attributes can be explained by the nutritional rich content of AGE including vitamin C, phytohormones, K, P, Mg, Ca, and Zn in garlic extract (Kasim et al. 2017b). Similarly, the use of biostimulants derived from plant extracts has been documented to stimulate plant growth and increase the levels of photosynthetic pigments (El-Shenody et al. 2023; Mohamed and Akladious 2014). Consequently, the biosynthetic pathways of photosynthetic pigments would be activated by offering their needed nutrients or limiting cellular As-toxicity following garlic extract application. The reduction in carotenoid levels observed in plants treated with AGE and As +AGE in comparison to control and As-stressed plants individually may be attributed to the protective function of AGE in mitigating chlorophyll oxidation and activity of photosystems. This protective mechanism helps prevent the diversion of plant metabolic pathways towards secondary metabolites, thereby conserving energy reserves and facilitating continued growth, even under stressful conditions.

Because of metal exposure, the As-induced physiological drought was followed by increased accumulation of osmolytes including total amino acids (TAA), free proline (FP), and glycine betaine (GB) as compared with control, which harmfully affected dry matter building up. The improved production of osmolytes could considerably contribute to metal tolerance and counterbalancing metal-induced water deficit (Ragab and Saad-Allah 2020). Among osmolytes, the maximum enhancement was recorded with FP levels. The overproduction of FP was reported in plants stressed by As due to its potent role as an osmoprotectant and non-enzymatic antioxidant. It maintains an adequate hydration level required for the normal functioning of the cell, acts as a cell wall plasticizer, and scavenges ROS-mediated damages (Abbas et al. 2018).

The pre-treatment of fenugreek seeds with AGE before their exposure to As stress significantly increased the leaf contents of TAA, FP, and GB as compared to the single As treatment, which could effectively integrate into vital tolerance responses. In this regard, plant defense strategies could be elicited by biostimulants as low-cost and sustainable strategies (Hayat et al. 2018b; Kasim et al. 2017a, 2019). The phytochemical analysis of AGE showed its richness of organic sulfur compounds and phenol-containing phytochemicals. In this context, the application of garlic extract significantly enhanced the osmolytes level in soybean water-stressed plants (Mohamed and Akladious 2014). The intensive accumulation of osmolytes would prevent the loss of turgidity and detoxify elevated ROS (Alhaithloul et al. 2022).

The irrigation with sodium arsenate induced a higher accumulation of As ions in *Trigonella* shoots and roots. The deposition of As in plant tissues induces significant malfunctions in physiological and biochemical functions (Jalil et al. 2023; Saleem et al. 2023). Due to its non-essentiality, As accumulation causes oxidative stress and tissue injury, harming cellular metabolism and membrane permeability (Xalxo et al. 2021). The As-stressed roots accumulated higher As levels than shoots, indicating restricted upper translocation and enhanced tolerance due to the roots' ability to fix toxic metal ions. Thereby, a distinct observation of As deposition was demonstrated in TEM micrographs of root cells rather than shoot. The direct interaction of plant roots

with a soil-polluted environment was reported to induce As immobilizing and compartmentalizing via vacuolar membrane transporters, hindering its transport and toxicity to the shoots (Hu et al. 2021).

An evident decrease in the levels of As in plant tissues (shoot and root) was detected after AGE priming, demonstrating an impairment in its uptake. The positive impact of AGE could be attributed to retaining the structural integrity of membranes, cellular osmotic strength, and managing water uptake. The AGE was previously reported to stimulate tomato growth and membrane permeability due to the enhanced antioxidant enzymes (Hayat et al. 2018b). In this regard, the lower uptake of As, upon AGE priming, is considered a central reason for the decreased ROS production and the increased photosynthetic performance and growth of fenugreek seedlings. Herne, the findings presented demonstrate the capacity of AGE to alter the quantity of bioaccessible As within the rhizosphere. This observation raises the possibility that treating with AGE could induce the immobilization of arsenic within the soil through the formation of complexes and/or chelates with As, thereby decreasing its bioavailability for uptake and subsequently diminishing the concentration of As within the root system. However, further investigations are necessary to evaluate the long-term effectiveness of AGE in modifying As uptake within the root system in polluted soils.

The exposure to As-polluted irrigation water resulted in a significant elevation of oxidative stress biomarkers including H_2O_2, $OH^{\bullet}$, and MDA levels. Like other redox-active metals, As contributes directly to Haber-Weiss and Fenton reactions inducing ROS generation and inhibiting metabolic pathways (Ragab and Saad-Allah 2021). The over-production of ROS is linked to the toxicity of highly accumulated As ions in fenugreek seedlings, causing membrane lipids peroxidation. Consistent with our results, As stress accumulated high levels of H_2O_2, $OH^{\bullet}$ causing oxidative damage of membrane lipids, thus increasing MDA contents in *Camellia sinensis* plants (Li et al. 2021). The direct consequence of As-induced oxidative stress is the activation of antioxidant enzymes including CAT, GPOX, GR, and PPO. The provoked antioxidative machinery can counteract oxidative stress and maintain cell redox homeostasis under heavy metal stress. Furthermore, the present results declared that As exposure triggered the contents of non-enzymatic antioxidants including ASA, GSH, flavonoids, and phenolics demonstrating their distinct participation in ROS scavenging (Karam et al. 2017).

Under conditions of metal stress, the improved functioning of antioxidant enzymes, which are responsible for the regulation of ROS accumulation and prevention of oxidative damage, proves to be inadequate in mitigating the toxic effects of As. The present study provides evidence supporting this hypothesis, as it demonstrates the occurrence of acute oxidative toxicity and suppression in the activities of SOD and APOX upon exposure to As. This phenomenon can be attributed to the potential of As to interact with and displace functional groups within enzymes, particularly sulfhydryl groups (Abbas et al. 2018). The diminished activity of APOX, primarily localized in chloroplasts, is believed to be a direct consequence of the compromised ultrastructure and integrity of chloroplasts under As-induced stress. Similar inactivation of APOX linked to oxidative toxicity has been observed in mung bean plants exposed to As stress (Singh et al. 2007). Furthermore, the impaired functioning of SOD and APOX can lead to the accumulation of elevated levels of $O_2^{\bullet-}$ and H_2O_2, while inhibiting the ASA–GSH scavenging cycle.

In comparison, AGE priming promoted the recovery of oxidative damage by stimulating both antioxidant enzymes and non-enzymatic antioxidants. The AGE priming treatment significantly enhanced the levels of ASA, GSH, flavonoids, and phenolics compared to both the stress and control treatments, hence attenuating the cellular toxicity caused by ROS. The pronounced enhancement in antioxidative machinery by AGE priming could limit ROS noxiousness and retain cellular metabolism under As stress thus improving plant growth and performance. In this regard, the AGE could exhibit a positive impact under stress and stimulate the antioxidant response when applied as bio-priming or foliar spraying (Ali et al. 2019; Hayat et al. 2018b). The garlic's bioactive organosulfur and phenolic compounds might act directly as antioxidants to restrict the deleterious impacts of ROS and As toxicity or endogenously metabolized. Therefore, it can be argued that AGE priming could supply the plant with sulfur (S), which is subsequently incorporated into redox-active cysteine residues and S compounds like GSH. In a particular way, the promotion of As-diminished SOD activity due to AGE is a considerable advantage as the first line of plant defense against ROS via elimination of $O_2^{\bullet-}$ yielding H_2O_2. Also, the stimulation of APOX activity can particularly operate the ASA–GSH cycle as a main component of H_2O_2 detoxification (Karam et al. 2017). The effective role of APOX depends on the presence of high levels of ASA induced by AGE treatment where it uses two ASA molecules to reduce H_2O_2 to water (Abbas et al. 2018). The restoration of As-upregulated activities of CAT and PPO was observed with AGE priming, indicating that either the promotion or suppression of enzymatic antioxidants takes place in conjugation with each other to combat toxic ROS levels. Thus, it may be inferred that AGE priming can upregulate the ASA–GSH cycle marked by the increased activities and contents of its contributing components.

When administered individually, As stress caused significant structural changes at the ultrastructural level in both the

leaves and roots of fenugreek seedlings. The TEM images showed significant subcellular damage, particularly affecting the development of the cell wall and several protoplasmic organelles such as chloroplasts, mitochondria, and the plasma membrane. In a particular way, chloroplasts showed high structural sensitivity to As toxicity with destructions in their outer double-lining membrane and internal membrane-bounded systems (Fig. 4F and G, and 4H). The structural damage of chloroplasts coincided with the physiological disorders in chloroplasts including chlorophyll depletion and inhibited photosynthetic activity suppressing photosynthesis and plant growth. The primary target of ROS cellular destruction, under metal toxicity, is assumed to be the chloroplast which alters the lipid composition of thylakoid membranes (Kasim et al. 2014). The entirely disrupted thylakoid membranes that appeared with dark electron-dense bodies of plastoglobuli (Fig. 4G and H) were greatly observed in As stress chloroplasts. During metal stress, the increased plastoglobuli, as lipoprotein deposits, could indicate the elevated breakdown of thylakoid membrane lipids (Panou-Filotheou 2001). Moreover, the selective permeability of the plasma membrane was harmed as evident by As-induced plasmolysis (Fig. 4F), as well as an increase in the levels of MDA. In similar reports, As-treated plants showed cell plasmolysis and swelling of chloroplasts with increased plastoglobuli (Karam et al. 2017; Li et al. 2006).

Plasma membrane vesiculation and cytoplasmic microvesicles have been observed as potential indicators of apoptosis and the initiation of cell death in response to As treatment. These disorders are mainly attributed to excessive ROS production and accumulation of As ions causing oxidative damage to membranes and cytoplasm leakage. The increased level of ROS can directly cause oxidation of various biomolecules and induce the denaturation of the cytosol (Jin et al. 2010). It has been reported that the high level of ROS could contribute to cell signaling cascade related to the modification and collapse of membranes via induction of specific enzyme processing systems (Li et al. 2012). The alterations in mitochondrial membranes due to As metal toxicity (Fig. 4F) would harmfully affect cellular respiration and plant carbon skeletons. Likewise, *Pistia stratiotes* leaf mesophyll tissues subjected to As stress had disrupted cellular structures such as chloroplast and mitochondria leading to possible programmed cell death. Meanwhile, the arsenate could compete with phosphate for the same active site of ATP synthase to yield an unstable product, thus uncoupling the oxidative phosphorylation, and disrupting the energy status of the cell (Farnese et al. 2017).

The priming with AGE considerably minimized the structural toxicity of As and retained the distinct cellular compartments. The intact thylakoid membranes and well-represented mitochondrial cristae were noticeable (Fig. 4I and J, and 4K) as pivotal recovery symptoms of As stress. Moreover, keeping the substantial cellular turgidity and complete disappearance of plasmolysis reflected the adjustment of the hydraulic status of the plant and the absence of cell apoptosis symptoms. This relieving capacity can be assumed to be a result of hindering ROS concentration and decreased As content. Garlic phytochemicals were found to induce antioxidant enzyme activities and defense responses in tomato plants with enhanced growth and development (Hayat et al. 2020).

Furthermore, ultrastructural changes in the root conducting system due to As exposure were marked by the distortion of the xylem lignification and water transport system. Moreover, the intercellular spaces of the root cortex accumulated dark dense vesicles of possible As deposits to restrict As uptake (Fig. 5G). The decreased relative water content and plant growth are principal evidence for disruption of the water transport system upon As treatment. As stress induced structural alterations in the roots' vascular system with dark deposits in the central cylinder and cortex which could be a detoxification strategy to limit As translocation in soybean seedlings (Armendariz et al. 2016). The cell wall structural damage was also observed in root cells at variable levels including thinning, detachment from the protoplasm, and appearance of nicks or amoeboid protrusions. Under stressful conditions, plants tend to increase cell wall surface area via folds and amoeboid extensions as an adaptive strategy to trigger water and ions transport (Kurkova et al. 2002). The toxicity of As could extend to attenuating metabolic processes related to the synthesis and disposition of cell wall microfibrils causing fold formation as previously suggested in Pb-stressed wheat roots (Kaur et al. 2013). The nucleus disintegration and condensed chromatin are acute toxicity symptoms detected under metal stress indicating DNA damage and oxidation (Kasim et al. 2014). These severe ultrastructural events significantly restricted plant growth and developmental stages.

As a result of priming with AGE, normal cellular structures in roots were restored including cell wall, nucleus, and xylem vessels construction while the intercellular spaces showed tiny dense depositions of As (Fig. 5J and K). The priming with AGE revealed a large nucleus in the root cells indicating both enhanced metabolic activity and impaired toxicity of As. In this context, AGE increased auxin biosynthesis and transport, expression patterns of defense-related genes, antioxidant enzyme activities, and phytohormonal regulations to promote stress resistance pathways (Hayat et al. 2020).

5 Conclusions

From the current findings, agricultural soil pollution with arsenate (As) can be highlighted with several toxicity symptoms in fenugreek seedlings including inhibited growth and photosynthesis, elevated oxidative stress biomarkers, restricted activities of antioxidant enzymes, and acute ultrastructural disorders. The significant effects of aqueous garlic extract (AGE) priming were significantly evident by relieving As-induced oxidative stress which is associated mainly with improved enzymatic and non-enzymatic antioxidants. AGE application hindered As uptake, which is closely related to the enhanced membrane permeability concomitant with the restoration of normal structural compartments. Hence, the nutritional value and the phytochemical composition of AGE priming offered enhanced antioxidative machinery and restricted As uptake with the physiological advantage of ultrastructure preservation to promote plant growth potential.

Supplementary Information The online version contains supplementary material available at https://doi.org/10.1007/s42729-025-02386-z.

Author Contributions Gehad A. Ragab: Conceptualization, Visualization, Methodology, Data curation, Software, Investigation, Writing-Original draft preparation, Writing- Reviewing and Editing. Khalil M. Saad-Allah: Conceptualization, Visualization, Methodology, Validation, Data curation, Investigation, Writing- Reviewing and Editing. Afaf A. Nessem: Conceptualization, Visualization, Methodology, Data curation, Software, Investigation, Writing- Original draft preparation, Writing- Reviewing and Editing.

Funding Open access funding provided by The Science, Technology & Innovation Funding Authority (STDF) in cooperation with The Egyptian Knowledge Bank (EKB).
No funding was received for conducting this study.

Declarations

Financial Interests The authors have no relevant financial or non-financial interests to disclose.

Conflict of Interest The authors declare no competing interest.

Open Access This article is licensed under a Creative Commons Attribution 4.0 International License, which permits use, sharing, adaptation, distribution and reproduction in any medium or format, as long as you give appropriate credit to the original author(s) and the source, provide a link to the Creative Commons licence, and indicate if changes were made. The images or other third party material in this article are included in the article's Creative Commons licence, unless indicated otherwise in a credit line to the material. If material is not included in the article's Creative Commons licence and your intended use is not permitted by statutory regulation or exceeds the permitted use, you will need to obtain permission directly from the copyright holder. To view a copy of this licence, visit http://creativecommons.org/licenses/by/4.0/.

References

Abbas G, Murtaza B, Bibi I, Shahid M, Niazi NK, Khan MI, Amjad M, Hussain M, Natasha (2018) Arsenic uptake, toxicity, detoxification, and speciation in plants: physiological, biochemical, and molecular aspects. Int J Environ Res Public Health 15:e59. https://doi.org/10.3390/ijerph15010059

Ahmad B, Dar TA, Khan MMA, Ahmad A, Rinklebe J, Chen Y, Ahmad P (2022) Oligochitosan fortifies antioxidative and photosynthetic metabolism and enhances secondary metabolite accumulation in arsenic-stressed peppermint. Front Plant Sci 13:e987746. https://doi.org/10.3389/fpls.2022.987746

Alaraidh IA, Alsahli AA, Abdel Razik ES (2018) Alteration of antioxidant gene expression in response to heavy metal stress in *Trigonella foenum-graecum* L. South Afr J Bot 115:90–93. https://doi.org/10.1016/j.sajb.2018.01.012

Alhaithloul HAS, Khan MI, Musa A, Ghoneim MM, Aysh ALrashidi A, Khan I, Azab E, Gobouri AA, Sofy MR, El-Sherbiny M, Soliman MH (2022) Phytotoxic effects of *Acacia saligna* dry leachates on germination, seedling growth, photosynthetic performance, and gene expression of economically important crops. PeerJ 10:e13623. https://doi.org/10.7717/peerj.13623

Ali M, Cheng Z, Hayat S, Ahmad H, Ghani MI, LIU T (2019) Foliar spraying of aqueous Garlic bulb extract stimulates growth and antioxidant enzyme activity in eggplant (*Solanum melongena* L). J Integr Agric 18:1001–1013. https://doi.org/10.1016/S2095-3119(18)62129-X

Alkharpotly AA, Abd-Elkader DY, Salem MZM, Hassan HS (2024) Growth, productivity and phytochemicals of coriander in responses to foliar application of *Acacia Saligna* fruit extract as a biostimulant under field conditions. Sci Rep 14:e2921. https://doi.org/10.1038/s41598-024-53378-5

Allen SE, Grimshaw HM, Parkinson JA, Quarmby C (1974) Chemical analysis of ecological materials. Blackwell Scientific., New York

Anderson ME, Andersen ME (1985) Determination of glutathione and glutathione disulphide in biological samples. Annu Rev Biochem 113:548–555. https://doi.org/10.1016/s0076-6879(85)13073-9

AOAC (1995) Official methods of analysis, 16th edn. Association of Official Analytical Chemists, Washington, DO

Armendariz AL, Talano MA, Travaglia C, Reinoso H, Wevar Oller AL, Agostini E (2016) Arsenic toxicity in soybean seedlings and their Attenuation mechanisms. Plant Physiol Biochem 98:119–127. https://doi.org/10.1016/j.plaphy.2015.11.021

Arnon DI (1949) Copper enzymes in isolated chloroplasts. Polyphenoloxidase in *Beta vulgaris*. Plant Physiol 24:1–15. https://doi.org/10.1104/pp.24.1.1

Bates LS, Waldren RP, Teare ID (1973) Rapid determination of free proline for water-stress studies. Plant Soil 39:205–207. https://doi.org/10.1007/BF00018060

Beyer WF, Fridovich I (1987) Assaying for superoxide dismutase activity: some large consequences of minor changes in conditions. Anal Biochem 161:559–566. https://doi.org/10.1016/0003-2697(87)90489-1

Bulgari R, Cocetta G, Trivellini A, Vernieri P, Ferrante A (2015) Biostimulants and crop responses: A review. Biol Agric Hortic 31:1–17. https://doi.org/10.1080/01448765.2014.964649

Chang C-C, Yang M-H, Wen H-M, Chern J-C (2002) Estimation of total flavonoid content in propolis by two complementary colorimetric methods. J Food Drug Anal 10:178–182. https://doi.org/10.38212/2224-6614.2748

Du L, Xia X, Lan X, Liu M, Zhao L, Zhang P, Wu Y (2017) Influence of arsenic stress on physiological, biochemical, and morphological characteristics in seedlings of two cultivars of maize (*Zea Mays* L). Water Air Soil Pollut 228:e55. https://doi.org/10.1007/s11270-016-3231-2

Dubois M, Gilles K, Hamilton J, Rebers P, Smith F (1965) Colorimetric method for determination of sugars and related substances. Anal Chem 28:350–356. https://doi.org/10.1021/ac60111a017

El-Shenody RA, Elshobary ME, Ragab GA, Huo S, Essa D (2023) Towards biorefinery: exploring the potential of seaweed-derived biodiesel and its residual biomass in improving the traits of *Eruca vesicaria* (L.) Cav. South Afr J Bot 155:361–371. https://doi.org/10.1016/j.sajb.2023.02.029

Farnese FS, Oliveira JA, Paiva EAS, Menezes-Silva PE, da Silva AA, Campos FV, Ribeiro C (2017) The involvement of nitric oxide in integration of plant physiological and ultrastructural adjustments in response to arsenic. Front Plant Sci 8:e516. https://doi.org/10.3389/fpls.2017.00516

Farouk S, Al-Amri SM (2019) Exogenous melatonin-mediated modulation of arsenic tolerance with improved accretion of secondary metabolite production, activating antioxidant capacity and improved Chloroplast ultrastructure in Rosemary herb. Ecotoxicol Environ Saf 180:333–347. https://doi.org/10.1016/j.ecoenv.2019.05.021

Fatima A, Kataria S, Prajapati R, Jain M, Agrawal AK, Singh B, Kashyap Y, Tripathi DK, Singh VP, Gadre R (2020) Magnetopriming effects on arsenic stress-induced morphological and physiological variations in soybean involving synchrotron imaging. Physiol Plant 173:88–99. https://doi.org/10.1111/ppl.13211

Gąsecka M, Drzewiecka K, Magdziak Z, Piechalak A, Budka A, Waliszewska B, Szentner K, Goliński P, Niedzielski P, Budzyńska S, Mleczek M (2021) Arsenic uptake, speciation and physiological response of tree species (*Acer Pseudoplatanus, betula pendula* and *Quercus robur*) treated with dimethylarsinic acid. Chemosphere 263:e127859. https://doi.org/10.1016/j.chemosphere.2020.127859

Golubkina N, Kharchenko V, Moldovan A, Antoshkina M, Ushakova O, Sękara A, Stoleru V, Murariu OC, Tallarita AV, Sannino M, Caruso G (2024) Effect of selenium and Garlic extract treatments of seed-addressed lettuce plants on biofortification level, seed productivity and mature plant yield and quality. Plants 13:e1190. https://doi.org/10.3390/plants13091190

Grieve CMM, Grattan SRR (1983) Rapid assay for determination of water soluble quaternary ammonium compounds. Plant Soil 70:303–307. https://doi.org/10.1007/BF02374789

Halliwell B, Foyer CH (1978) Properties and physiological function of a glutathione reductase purified from spinach leaves by affinity chromatography. Planta 139:9–17. https://doi.org/10.1007/BF00390803

Hayat S, Ahmad H, Ali M, Hayat K, Khan MA, Cheng Z (2018a) Aqueous Garlic extract as a plant biostimulant enhances physiology, improves crop quality and metabolite abundance, and primes the defense responses of receiver plants. Appl Sci 8:e1505. https://doi.org/10.3390/app8091505

Hayat S, Ahmad H, Ali M, Ren K, Cheng Z (2018b) Aqueous Garlic extract stimulates growth and antioxidant enzymes activity of tomato (*Solanum lycopersicum)*. Sci Hortic 240:139–146. https://doi.org/10.1016/j.scienta.2018.06.011

Hayat S, Ahmad H, Nasir M, Khan MN, Ali M, Hayat K, Khan MA, Khan F, Ma Y, Cheng Z (2020) Some physiological and biochemical mechanisms during seed-to-seedling transition in tomato as influenced by Garlic allelochemicals. Antioxidants 9:e235. https://doi.org/10.3390/antiox9030235

Heath RLRL, Packer L (1968) Photoperoxidation in isolated chloroplasts: I. Kinetics and stoichiometry of fatty acid peroxidation. Arch Biochem Bophysics 125:189–198. https://doi.org/10.1016/0003-9861(68)90654-1

Horvath G, Kissimon J, Faludi-Dániel Á (1972) Effect of light intensity on the formation of carotenoids in normal and mutant maize leaves. Phytochemistry 11:183–187. https://doi.org/10.1016/S0031-9422(00)89987-2

Hossain MA, Shah MD, Sakari M (2011) Gas chromatography–mass spectrometry analysis of various organic extracts of *Merremia Borneensis* from Sabah. Asian Pac J Trop Med 4:637–641. https://doi.org/10.1016/S1995-7645(11)60162-4

Hu L, Wang X, Wu D, Zhang B, Fan H, Shen F, Liao Y, Huang X, Gao G (2021) Effects of organic selenium on absorption and bioaccessibility of arsenic in radish under arsenic stress. Food Chem 344:e128614. https://doi.org/10.1016/j.foodchem.2020.128614

Jalil S, Alghanem SMS, AL-Huqail AA, Nazir MM, Zulfiqar F, Ahmed T, Ali S, Abeed HA, Siddique A, Jin KHM X (2023) Zinc oxide nanoparticles mitigated the arsenic induced oxidative stress through modulation of physio-biochemical aspects and nutritional ions homeostasis in rice (*Oryza sativa* L). Chemosphere 338:e139566. https://doi.org/10.1016/j.chemosphere.2023.139566

Jin J-W, Xu Y-F, Huang Y-F (2010) Protective effect of nitric oxide against arsenic-induced oxidative damage in tall fescue leaves. Afr J Biotechnol 9:1619–1627. https://doi.org/10.5897/AJB10.1442

Jindal KK, Singh RN (1975) Phenolic content in male and female *Carica papaya*: A possible physiological marker for sex identification of vegetative seedlings. Physiol Plant 33:104–107. https://doi.org/10.1111/j.1399-3054.1975.tb03774.x

Karam EA, Keramat B, Sorbo S, Maresca V, Asrar Z, Mozafari H, Basile A (2017) Interaction of Triacontanol and arsenic on the ascorbate-glutathione cycle and their effects on the ultrastructure in *Coriandrum sativum* L. Environ Exp Bot 141:161–169. https://doi.org/10.1016/j.envexpbot.2017.07.012

Kasim WA, Abokassem EM, Ragab GA, Sewelam NA (2014) Alleviation of lead stress toxicity in vigna unguiculata by Salicylic acid. Egypt J Exp Biol 10:37–49. https://doi.org/https://www.egyseb.net/fulltext/15-1429962130.pdf

Kasim W, AboKassem E, Ragab G (2017a) Ameliorative effect of yeast extract, IAA and green-synthesized nano zinc oxide on the growth of Cu-stressed *Vicia Faba* seedlings. Egypt J Bot 57:1–16. https://doi.org/10.21608/ejbo.2017.885.1065

Kasim W, Nessem EA, Gaber A (2017b) Alleviation of drought stress in *Vicia Faba* by seed priming with ascorbic acid or extracts of Garlic and Carrot. Egypt J Bot 57:45–59. https://doi.org/10.21608/ejbo.2017.831.1057

Kasim WA, Nessem AA, Gaber A (2019) Effect of seed priming with aqueous extracts of Carrot roots, Garlic cloves or ascorbic acid on the yield of *Vicia Faba* grown under drought stress. Pakistan J Bot 51:1979–1985. https://doi.org/10.30848/PJB2019-6(41)

Kato M, Shimizu S (1987) Chlorophyll metabolism in higher plants. VII. Chlorophyll degradation in senescing tobacco leaves; phenolic-dependent peroxidative degradation. Can J Bot 65:729–735. https://doi.org/10.1139/b87-097

Kaur S, Singh HP, Batish DR, Negi A, Mahajan P, Rana S, Kohli RK (2012) Arsenic (As) inhibits radicle emergence and elongation in *Phaseolus aureus* by altering starch-metabolizing enzymes vis-à-vis disruption of oxidative metabolism. Biol Trace Elem Res 146:360–368. https://doi.org/10.1007/s12011-011-9258-8

Kaur G, Singh HP, Batish DR, Kohli RK (2013) Lead (Pb)-induced biochemical and ultrastructural changes in wheat (*Triticum aestivum*) roots. Protoplasma 250:53–62. https://doi.org/10.1007/s00709-011-0372-4

Kumar KB, Khan PA (1982) Peroxidase and polyphenol oxidase in excised ragi (*Eleusine Corocana* Cv PR 202) leaves during senescence. Indian J Exp Biol 20:412–416

Kurkova EB, Myasoedov NA, Kotov AA, Kotova LM, Lun'kov RV, Shamsutdinov NZ, Balnokin Y (2002) Specific structure of root cells of the salt-accumulating halophyte *Suaeda altissima* L. Dokl Biol Sci 387:573–576. https://doi.org/10.1023/a:1021710128974

Kutasy B, Kiniczky M, Decsi K, Kálmán N, Hegedűs G, Alföldi ZP, Virág E (2023) Garlic-lipo'4Plants: Liposome-encapsulated

Garlic extract stimulates ABA pathway and PR genes in wheat (*Triticum aestivum*). Plants 12:e743. https://doi.org/10.3390/plants12040743

Lee YYP, Takahashi T (1966) An improved colorimetric determination of amino acids with the use of ninhydrin. Anal Biochem 14:71–77. https://doi.org/10.1016/0003-2697(66)90057-1

Li W-X, Chen T-B, Huang Z-C, Lei M, Liao X-Y (2006) Effect of arsenic on Chloroplast ultrastructure and calcium distribution in arsenic hyperaccumulator *Pteris* vittata L. Chemosphere 62:803–809. https://doi.org/10.1016/j.chemosphere.2005.04.055

Li Z, Yue H, Xing D (2012) MAP kinase 6-mediated activation of vacuolar processing enzyme modulates heat shock-induced programmed cell death in Arabidopsis. New Phytol 195:85–96. https://doi.org/10.1111/j.1469-8137.2012.04131.x

Li Q, Wang HH, Wang HH, Zheng W, Wu D, Wang Z (2018) Effects of Kinetin on plant growth and Chloroplast ultrastructure of two *Pteris* species under arsenate stress. Ecotoxicol Environ Saf 158:37–43. https://doi.org/10.1016/j.ecoenv.2018.04.009

Li X, Ahammed GJ, Zhang XN, Zhang L, Yan P, Zhang LP, Fu JY, Han WY (2021) Melatonin-mediated regulation of anthocyanin biosynthesis and antioxidant defense confer tolerance to arsenic stress in *Camellia sinensis* L. J Hazard Mater 403:e123922. https://doi.org/10.1016/j.jhazmat.2020.123922

Luziatelli F, Ficca AG, Colla G, Švecová EB, Ruzzi M (2019) Foliar application of vegetal-derived bioactive compounds stimulates the growth of beneficial bacteria and enhances Microbiome biodiversity in lettuce. Front Plant Sci 10:e60. https://doi.org/10.3389/fpls.2019.00060

Mishra RK, Tiwari S, Patel A, Prasad SM (2021) Arsenic contamination, speciation, toxicity and defense strategies in plants. Rev Bras Bot 44:1–10. https://doi.org/10.1007/s40415-020-00694-5

Mohamed HI, Akladious SA (2014) Influence of Garlic extract on enzymatic and Non enzymatic antioxidants in soybean plants (*Glycine max*) grown under drought stress. Life Sci J 11:46–58

Nakano Y, Asada K (1981) Hydrogen peroxide is scavenged by ascorbate-specific peroxidase in spinach chloroplasts. Plant Cell Physiol 22:867–880

NIST N (2014) EPA/NIH mass spectral library. In: Natl. Inst. Stand. Technol. Gaithersbg. http://www.nist.gov/srd/nist1a.cfm#. Accessed 5 Oct 2022

Oberacher H (2012) Wiley registry of tandem mass spectral data, MS for ID. John Wiley & Sons Inc, Hoboken, NJ, USA, Hoboken

Oser BL (1979) Hawk's physiological chemistry, 14th edn. McGraw-Hills, New York

Panou-Filotheou H (2001) Effects of copper toxicity on leaves of oregano (*Origanum vulgare* subsp. hirtum). Ann Bot 88:207–214. https://doi.org/10.1006/anbo.2001.1441

Ragab GAGA, Saad-Allah KMKM (2020) Green synthesis of sulfur nanoparticles using *Ocimum Basilicum* leaves and its prospective effect on manganese-stressed *Helianthus annuus* (L.) seedlings. Ecotoxicol Environ Saf 191:110242. https://doi.org/10.1016/j.ecoenv.2020.110242

Ragab G, Saad-Allah K (2021) Seed priming with Greenly synthesized sulfur nanoparticles enhances antioxidative defense machinery and restricts oxidative injury under manganese stress in *Helianthus annuus* (L.) seedlings. J Plant Growth Regul 40:1894–1902. https://doi.org/10.1007/s00344-020-10240-y

Rai PK, Song H, Kim KH (2023) Nanoparticles modulate heavy-metal and arsenic stress in food crops: hormesis for food security/safety and public health. Sci Total Environ 902:e166064. https://doi.org/10.1016/j.scitotenv.2023.166064

Reynolds ES (1963) The use of lead citrate at high pH as an electron-opaque stain in electron microscopy. J Cell Biol 17:208–212. https://doi.org/10.1083/jcb.17.1.208

Saad-Allah KM, Ragab GA (2020) Sulfur nanoparticles mediated improvement of salt tolerance in wheat relates to decreasing oxidative stress and regulating metabolic activity. Physiol Mol Biol Plants 26:2209–2223. https://doi.org/10.1007/s12298-020-00899-8

Saleem K, Asghar MA, Javed HH et al (2023) Alleviation of arsenic toxicity-induced oxidative stress in lemon grass by Methyl jasmonate. South Afr J Bot 160:547–559. https://doi.org/10.1016/j.sajb.2023.07.034

Seleem EM, Mostafa A, Mokhtar M, Salman SA (2021) Risk assessment of heavy metals in drinking water on the human health, Assiut City, and its environs, Egypt. Arab J Geosci 14:e427. https://doi.org/10.1007/s12517-021-06784-2

Sharma HSS, Fleming C, Selby C, Rao JR, Martin T (2014) Plant biostimulants: a review on the processing of macroalgae and use of extracts for crop management to reduce abiotic and biotic stresses. J Appl Phycol 26:465–490. https://doi.org/10.1007/s10811-013-0101-9

Sharma DK, Dave RS, Shah KR (2022) Proximate analysis, preliminary phytochemical screening and characterization of compounds by GC–MS from *Cycas revoluta*. Vegetos 35:756–762. https://doi.org/10.1007/s42535-021-00338-3

Shindy WW, Smith OE (1975) Identification of plant hormones from cotton ovules. Plant Physiol 55:550–554. https://doi.org/10.1104/pp.55.3.550

Singh HP, Batish DR, Kohli RK, Arora K (2007) Arsenic-induced root growth Inhibition in mung bean (*Phaseolus aureus* Roxb.) is due to oxidative stress resulting from enhanced lipid peroxidation. Plant Growth Regul 53:65–73. https://doi.org/10.1007/s10725-007-9205-z

Thakur S, Choudhary S, Majeed A, Singh A, Bhardwaj P (2020) Insights into the molecular mechanism of arsenic phytoremediation. J Plant Growth Regul 39:532–543. https://doi.org/10.1007/s00344-019-10019-w

Tufail M, Hussain K, Iqbal I, Nawaz K, Arshad N, Jafar S, Arif U (2020) Efficacy of IAA, GA3 and riboflavin for morpho-biochemical and yield attributes of Fenugreek (*Trigonella foenum-graecum* L.) in Pakistan. Legum Res 43:780–787. https://doi.org/10.18805/A-575

Velikova V, Yordanov I, Edreva A (2000) Oxidative stress and some antioxidant systems in acid rain-treated bean plants. Plant Sci 151:59–66. https://doi.org/10.1016/S0168-9452(99)00197-1

Whitley E, Ball J (2002) Statistics review 6: nonparametric methods. Crit Care 6:509. https://doi.org/10.1186/cc1820

Xalxo R, Keshavkant S (2020) Growth and antioxidant responses of *Trigonella foenum-graecum* L. seedlings to lead and simulated acid rain exposure. Biologia 75:1115–1126. https://doi.org/10.2478/s11756-020-00478-y

Xalxo R, Chandra J, Pandey N, Sahu K (2021) Physiological and molecular mechanism of metalloid tolerance in plants. In: Hasanuzzaman M (ed) Approaches to the remediation of inorganic pollutants. Springer Singapore, Singapore, pp 197–221

Yadav P, Ansari MW, Gill R, Tuteja N, Gill SS (2024) Arsenic transport, detoxification, and recent technologies for mitigation: a systemic review. Plant Physiol Biochem 213:e108848. https://doi.org/10.1016/j.plaphy.2024.108848

Zulfiqar F, Casadesús A, Brockman H, Munné-Bosch S (2020) An overview of plant-based natural biostimulants for sustainable horticulture with a particular focus on Moringa leaf extracts. Plant Sci 295:e110194. https://doi.org/10.1016/j.plantsci.2019.110194

Publisher's Note Springer Nature remains neutral with regard to jurisdictional claims in published maps and institutional affiliations.